Analysis of steady state Cryogenic Air Separation unit of Rourkela Steel Plant and simulation of Fixed Bed Adsorption Separation of Air

A thesis submitted towards partial fulfilment of the requirements for the degree of

Master of Technology

In

Mechanical Engineering

(Specialization: Cryogenics and Vacuum Technology)

By

Lukesh Kumar

Roll No. - 212ME5406

Department of Mechanical Engineering

National Institute of Technology

Rourkela-769008, Odisha

June 2014

Analysis of steady state Cryogenic Air Separation unit of Rourkela Steel Plant and simulation of Fixed Bed Adsorption Separation of Air

A thesis submitted towards partial fulfilment of the requirements for the degree of

Master of Technology

In

Mechanical Engineering

(Specialization: Cryogenics and Vacuum Technology)

By

Lukesh Kumar

Roll No. - 212ME5406

Under the supervision of

Prof. Basudeb Munshi

(Chemical Engineering Department)

Department of Mechanical Engineering

National Institute of Technology

Rourkela-769008, Odisha

June 2014

National Institute of Technology Rourkela

CERTIFICATE OF APPROVAL

This is to certify that the abstract entitled "**Analysis of steady state Cryogenic Air Separation unit of Rourkela Steel Plant and simulation of Fixed Bed Adsorption Separation of Air",** being submitted by **Mr. Lukesh Kumar**, Roll No. 212ME5406 in the partial fulfillment of the requirements for the award of the Degree of Master of Technology in Mechanical Engineering, is a research carried out by him at the department of mechanical engineering**,** National Institute of Technology Rourkela and Rourkela steel plant, under our guidance and supervision.

The result presented in this abstract has not been, to the best of my knowledge, submitted to any other university or institute for the award of any degree. The abstract in our opinion has reached the standards fulfilling the requirement for the award of the degree of Master of Technology in accordance with regulations of the institute.

Supervisor

Date:

Prof. Basudeb Munshi

Associate Professor

Department of Chemical Engineering

National Institute of Technology, Rourkela

ACKNOWLEDGEMENT

I wish to express my sincere gratitude to my supervisor **Prof. B. Munshi,** for giving me an opportunity to work on this project, for his guidance, encouragement and support throughout this work and my studies here at NIT Rourkela. His impressive knowledge, technical skills and human qualities have been a source of inspiration and a model for me to follow.

I am grateful to **Prof. S. K. Sarangi**, Director, NIT Rourkela and **Prof. K.P. Maithy**, HOD, Department of Mechanical Engineering, and also the other staff members of Department of Mechanical Engineering, NIT Rourkela for providing me the necessary facilities that is required to conduct the experiment and complete my thesis.

I would like to thank to **Mr. C. R. Mohapatra**, (DGM TOP II), **Mr. Ashish Ranjan**, **Mrs. Kanchan Chaudhary** and **Mr. Sachine Bagdhe**, Rourkela Steel Plant, providing information about Air Separation process and valuable suggestion during entire work.

I am deeply indebted to my parents who always believed me and gave all their support for all the choices that I have made. Finally, I humbly bow my head with utmost gratitude before the God Almighty who always showed me a path to go and without whom I could not have done any of these.

Date:

Lukesh Kumar
Roll. No. - 212ME5406
Cryogenics and Vacuum Technology
Department of Mechanical Engineering
National Institute of Technology Rourkela

CONTENTS

ABSTRACT

Atmospheric dry air contains approximately 78% nitrogen, 21% oxygen, and 1% argon plus low concentrations of noble gases like carbon dioxide, hydrocarbons and other impurities. An air separation unit divides atmospheric air into the three pure gaseous components (nitrogen, oxygen and argon). Further separation may be performed on some plants to produce other gases such as krypton, neon and xenon. Other gas components of atmospheric air, such as carbon dioxide, water vapour and hydrocarbons must be removed to ensure safety, product quality and efficient plant operation. Nitrogen, oxygen and argon are used by industry in large quantities and hence termed industrial gases. The current work aim is to simulate the cryogenic air separation unit including adsorber and cryogenic distillation. Simulation of absorber is carried out using ADSIM of Aspen Tech to remove carbon dioxide (CO_2) and water vapour (H_2O). The breakthrough curves of carbon dioxide (CO_2) and water vapour on 5A molecular sieve and activated alumina respectively are found at different Reynolds number. The study helps to find out schedule time adsorber/desorber unit. ASPEN Plus simulator is used to simulate cryogenic air separation into nitrogen, oxygen and argon. The steady-state simulation results (purity) are compared to Rourkela steel plant real data.

Keywords: *Cryogenic, distillation column, Pressure Swing adsorption, Aspen plus, Aspen Dynamics, Aspen Adsim, Steady state simulation, Composition, molecular sieve, activated alumina, isotherm parameter.*

LIST OF FIGURE

LIST OF TABLE

CHAPTER 1

INTRODUCTION

1.1. Background

1.2. Aim and objectives

1.1. Background

Over 3,000 air separation plants in 80 countries, 500 of them have been made in the last 15 years. The History of air separation has long time;

- In **1895** World´s first air liquefaction plant on a commercial scale, production scale, pilot plant scale,
- **1902** World's first air separation plant for the recovery of oxygen
- **1904** World's first air separation plant for the recovery of nitrogen
- **1910** World's first air separation plant using the double column rectification process,
- **1954** World's first air separation plant with air purification by means of absorbers
- **1978** Internal compression of oxygen is applied to tonnage air separation plants
- **1984** World's largest VAROX air separation plant with variable oxygen demand adjustment
- **1990** World's first tale-controlled air separation plant with unmanned operation, Pure argon production by rectification column
- **1991** World's largest air separation plant with packed columns
- **1992** Air separation plants produce mega pure gases, and
- **1997** Lined sets a new milestone in air separation history.

The first application of computer control an air separation plant was done in the early 1970s. Since that time, best advanced control technologies have been useful to improve the productivity and efficiency of air separation plant [1].

The components presented in air (Oxygen, Nitrogen, Argon etc.) are very often useful components in chemical technology. The biggest marketplaces for oxygen are in primary metals production, gasification and chemicals, petroleum refineries, concrete and glass products, clay and welding. Gaseous nitrogen (N_2) is used in the petroleum and chemical industries and it is also used widely by the metals industries and electronics for its inert properties. Liquid nitrogen (LN_2) is used in applications ranging from food freezing to cryogenic grinding of plastics. Argon, the third key constituent of air, uses as mostly in steelmaking, heat treating, welding, and manufacturing procedures for electronics.

Techniques such as Membrane, PSA (Pressure Swing Adsorption) and VPSA (vacuum Pressure Swing Adsorption), are normally used to separate a single constituent from normal

air. The only possible sources of the rare gases krypton, xenon, and neon are the distillation of air using at least two distillation columns.

1.2. Aim and objectives

The overall aim of this research is described below:

1. Simulate the air separation unit of Rourkela steel plant (RSP) in steady state including adsorber and cryogenic distillation to produce pure nitrogen, oxygen and argon with a purity level above to 99% from atmospheric air with the help of ASPEN Plus
2. Compare the result (purity percentage) of simulated steady state cryogenic air separation unit with Rourkela steel plant (RSP) real data.
3. Simulation of absorber is carried out using ADSIM of Aspen Tech to remove carbon dioxide (CO_2) and water vapour (H_2O). The breakthrough curves of carbon dioxide (CO_2) and water vapour on 5A molecular sieve and activated alumina respectively are found at different Reynolds number. The study helps to find out schedule time adsorber/desorber unit.

The following specific features shall highlight the capability of the plant as well as the design.

1. Energy-optimized process with internal compression oxygen.
2. External nitrogen compression for the nitrogen products.
3. High efficiency, multistage compression systems are used for the gas compression. The compressed gas is cooled after each compressor stage in order to approach isothermal compression as close as possible.
4. Molecular sieve adsorbers equipped with molecular sieve filling according to the latest technology retain water vapour, CO2, acetylene, propylene, butane and butylene.
5. Cascade condenser provides low pressure drops and small temperature differences, which results in low power consumption.
6. A state of the art column system containing a pressure column and a low pressure column is used. This includes the advantages of a low power consumption and improved oxygen recovery.
7. Argon separation is achieved entirely by cryogenic rectification.

CHAPTER 2

LITERATURE REVIEW

2.1. Introduction

2.2. Type of air separation and comparisons

2.3. Available literatures on cryogenic air separation process and adsorber

2.1. Introduction

Air at lower temperatures (-196°C) converts in liquid and so we can do the distillation or purification of the air into its pure components. Distillation of air is presently the most frequently used method for production of pure nitrogen (N_2), oxygen (O_2) and argon (Ar) on an industrial scale. Huge quantities of industrial gases such as nitrogen (N_2), oxygen (O_2), argon (Ar) and other rare gases are essential by almost all types of industries to run their production processes. Industry examples are metals and semiconductors, machinery and pulp, paper, chemical and petrochemical etc.

Atmospheric air exists as cost free raw material with its components of nitrogen 78%, oxygen 21% and less amounts of argon 0.9% by volume and other rare gases. Today cryogenic air separation principle forms the base of most of the plants, which, however, have been further optimized regarding variable product scope and energy consumption. The level of product purity varies and ranges from approximately 99.9 to 99.8%. All air separation plants work one of two types of process technology;

- Air separation at very low temperatures to liquefy the air and to produce the desired products by cryogenic process based on differences in boiling points, and
- Air separation at higher pressure using adsorption effects based on differences in specific properties of the gases (pressure swing adsorption, PSA).

Some constituents of atmospheric air (CO2, hydrocarbons, humidity) would damage the air separation plant and are therefore removed in the first stage of the plant by passing through filters, molecular sieves and coolers. Therefore the process air must be analyzed for traces of hydrocarbons. Moreover the cryogenic air separation process two another principles exist, pressure swing adsorption (adsorption effects) or membrane separation (gas permeability).

Ensuring product quality and reducing production costs (energy consumption) are dominating goals in air separation plant operation. The process medium is continuously checked for traces of hydrocarbons to optimize and to a trouble-free plant operation. Process gas analyzers are used throughout the process to provide the required data.

2.2. Type of air separation and comparisons

There are many type of air separation process, described in table 2.1.

Table 2.1: Comparisons between different types of air separation [2]

Process	Status	Byproduct Capability	Purity Limit (Vol. %)	Start-up Time
Cryogenic	Mature	Excellent	>99	Hours
Adsorption	Semi-mature	Poor	93-95	Minutes
Membrane	Semi-mature	Poor	40	Minutes
Chemical	Developing	Poor	>99	Hours
ITM	Developing	Poor	>99	Hours

2.3 Available literatures on cryogenic air separation process and adsorber

H. Juma et al. [3] shows steady-state and dynamic simulation in a crude oil distillation plant was performed using ASPEN plus and Steady-state simulation results gotten by ASPEN plus were compared to experimental data. Simulations curves were compared to the experimental ASTM D86 curves of different products. Steady-state flow sheet was done by dynamic simulation and exported to ASPEN Dynamics for simulations in dynamic mode.

Y. Liwei et al. [4] presented the new air separation process for energy saving. The actual operating performance is analyzed for the total site. The optimization of such process can be solved by a novel algorithm in which the multi-objective genetic algorithm and linear programming are combined. Therefore the problem with multi-objective, multi-constraint and integers mixed will become easier to be studied. According to the simulation results, exergy efficiency of major equipment is analyzed. The equipment deficiency is overcome in the new process. Finally seven unified principles for energy saving, which can be widely used in air separation process, are summarized.

R. Agrawal et al. [5] have focuses on cryogenic process cycles to producing medium pressure N_2 at relatively high purity. This paper described an evolution of more efficient cryogenic N_2 generators to produce pressurized N_2.

C. Harry [6] have presented with the help of modern double column low pressure air separation cycle, a new process of cryogenic air separation has been developed. This paper focuses upon production of moderate pressure gaseous N_2 and high fractional recovery of argon. The M-Plant cycle, is created by the innovation of utilizing liquid O_2 to operate the crude argon column condenser rather than conventional oxygen-enriched kettle liquid. This novelty provides a favorable oxygen/argon (O_2/Ar) stripping reflux ratio in the lower portion of the low pressure column (upper column) and also inverts product pressures so that product pressure energy is retained in the larger N_2 fraction of the separated compressed air. The low pressure column (top column) operating conditions result up to 5 % more argon recovery compare to the traditional T-Plant cycle, and the N_2 product pressure inversion can result up to 10 % energy saving.

Z. Yu et al. [7] defined the problem of determining an optimum operating strategy to increase or maximize the total earning of a cryogenic air separation plant process while considering demand contractual obligations and uncertainty. To determine operating strategies, the use of rigorous optimization tools is important to allow effective decision making for any complex chemical process and to improve profitability.

Z. Yu et al. [8] shows effective design can reduce energy consumption and improve efficiency. This paper shows design of a cryogenic air separation plant process under uncertainty. The design from the multi scenario approach is related over the optimal design by using parameter values. To treatment of uncertainty in optimization, a popular approach is Multi-scenario programming. This paper includes greater than 675,000 variables and 196 scenarios, in the largest multi-scenario problem.

L.V. van der Ham [9] had studied the efficiency of a two column cryogenic air separation process is a part of an integrated gasification combined cycle can be increases significantly by improving the heat integration and by making well use of the heat of compression of the distillation column.

R. L. Cornelissen et al. [10] analyses that the exergy analysis of the cryogenic air distillation unit has quantified and pinpointed the exergy harm in the different plant divisions. The biggest amount of exergy loss is affected by the compressors. By using better compressors this exergy loss can be minimized a half.

L.V. van der Ham et al. [11] had studied two process designs of a cryogenic air separation unit (ASU) have been calculated using exergy analysis. A three and two column designs of a cryogenic air separation unit have been calculated using exergy analysis. Both designs were splitting the same feed into products with the same conditions. The 3 column design performed better than the two column design. This means that the three column design ruined 12 % less exergy.

J. Rizk et al. [12] have presented optimum configurations for least total exergy losses of 3 types of cryogenic distillation columns are evaluated. The columns considered for the comparison are the double adiabatic column, the simple adiabatic column, and the diabatic column (internally heat-integrated column). The double diabatic column shows 23% less exergy losses compare to the double adiabatic column.

F. Chao et al. [13] states that, when a double column distillation cycle is applied to produce oxygen with a pureness of 95mol %, the O2 production process is causing the highest power penalty compared to carbon dioxide (CO2) capture. This paper defines a comprehensive exergy study of an air separation plant for producing oxygen with low purity and low pressure. The distillation system and the air compression process cause the two largest exergy losses: 28.2% and 38.4% respectively. If the isentropic efficiency increases from 0.74 to 0.9 then power consumption in the air compressor can be reduced by 19%. When dual reboilers are used in the low pressure column then total power consumption is reduced by 10%.

J. Dustin et al. [14] considers five different configurations of an air separation unit with PLOX cycle and relates their power consumptions with an EP-ASU with a traditional gaseous oxygen cycle. The study indicate that an optimally designed EP-ASU with a PLOX cycle can have similar power consumption to that of an EP-ASU with GOX cycle in the case of 100 % N_2 integration. This paper compares the power savings in an LP-ASU with a PLOX cycle to the power savings in an EP-ASU with PLOX cycle and EP-ASU with GOX cycle. The results indicate that an LP-ASU with a PLOX cycle has less power consumption if the N_2 integration levels are less than 50–60 %. The study indicates that when the N_2 injection rate exceeds 50 %, an EP-ASU with a PLOX cycle is a well option than an LP-ASU with a PLOX cycle. This paper shows that an optimal integration and design of an air separation unit with the balance of the plant can help to rise the net power generation from an IGCC plant with carbon dioxide (CO2) capture.

E. Nobuaki et al. [15] states that, discussions on the effects of the vapor–liquid ratio in the feeds to the low pressure column the, the liquid-feed location to the low pressure column, and side-cut location to the argon column for a commercial scale cryogenic air separation plant are made by applying the simulator to show that there exist optimal values for these parameter.

Z. Lingyu et al. [16] have proposed a homotopy based backtracking method for the optimization and simulation of ASU. Furthermore, the changing load optimization result indicates that a large number of operating points that failed to converge with traditional algorithms could be successfully optimized with the HBM. Further analysis indicated that this technique also helped to trace the border of physical feasibility for product mix.

K. Yasuki et al. [17] had studied simulation studies specify that the proposed cryogenic air separation process with self-heat recuperation can decrease energy depletion by more than 36% related with a conventional cryogenic air separation process.

X. Zuhua et al. [18] developed an automatic load variation system of cryogenic air separation process to meet large variations in product demand from consumers. Industrial application results exhibit that this automatic load change system with a two-layer framework design can significantly reduce the O_2 release ratio and unit electricity consumption of air separation unit.

A.R. Smith et al. [19] had studied a review of developing and traditional processes to produce O_2 is presented, along with integration schemes to develop the economics of these facilities.

F. Chao et al. [20] have used vapor recompression heat pumps in distillation processes to reduce energy consumption. A scheme of recuperative vapor recompression heat pumps is developed to substitute the thermally coupled distillation columns, and this scheme is applied in cryogenic air separation processes in this paper. The power consumption has been significantly reduced compared to conventional double-column distillation cycles, and further reduced when the principle of distributed reboiling is applied to reduce irreversibilities in distillation columns. Two well-known energy saving technologies for distillation are applied and combined; vapor recompression and distributed reboiling.

D. R. Vinson [21] had studied achieving HPPC (high performance process control) requires that the control system operate the plant at optimum efficiency over the full range of dynamic and steady state conditions. The high performance process control challenges for both adsorption and cryogenic processes are presented, currently applicable research is concised, and guidelines for upcoming research are proposed. The value of the operability index to improved high performance process control is also discussed and presented.

T. Li et al. [22] have defined a typical air separation process is reconsidered for production scheduling by taking the future profiles of these important factors into account without uncertainty. A combined RTO and scheduling strategy is proposed based on the characteristics of air separation processes to optimize the total profit margin in a certain time horizon. In the paper, the special features of the scheduling problem of a typical ASU process producing both gas and liquid are presented, including the formulation of special constraints commonly seen in such a scheduling problem. The optimization feature and corresponding solution strategy are discussed.

Y. Fei et al. [23] performed an isotherm of n-pentane and n-hexane on 5A molecular sieve are identical to Langmuir fitting curves, and the fitting degrees are higher than 98%. Breakthrough curves are in good agreement with the experimental results, the deviation values of breakthrough time between simulation and experiment r less than 7% in single tower. At stable states, the breakthrough time of n-pentane is about 210s and n-hexane is about 420s, high purity (more than 95.5%wt iso-paraffins and more than 99.5%wt n-paraffins) products have been produced.

P. Jong et al. [24] states that, in order to achieve design data for pressure swing adsorption for H_2 (hydrogen) purification from the feed gas composed of CH4/H2/CO/CO_2, the adsorber dynamics in the double layered column were probed by both simulation and experiment. Both kinetic rollups and equilibrium are observed and their origins debated. Both model and experiment prediction tell that a double layered bed of zeolite and activated carbon can decrease the size of adsorber related to a single adsorbent bed of activated carbon.

M. Sampatrao et al. [25] performed that, experimental adsorption dynamic studies of EA adsorption on molecular sieves 13X and 5A display that equilibrium adsorption capability of EA in 13X is behaves closer to ideal behavior and it higher than 5A and MTZ (mass transfer zone) is well contained within the bed because of higher affinity of both the sieves for EA.

Mathematical model deprived of axial dispersion of mass and heat predicted the experimental results of dynamic adsorption of EA on 13X very well. Initial concentration breakthrough with higher inlet EA concentration, constant pattern breakthrough curves with the changes of inlet bed length, saturation adsorption capacity and velocity are observed.

S. W. Rutherford et al. [26] talk about analysis of kinetics and equilibrium of batch adsorption has presented that the characterized by the Darken relation, micropore diffusion, is rate limiting the dynamics of uptake in small Takeda 5A pellets.

Z. Junfang et al. [27] studied that adsorption of carbon dioxide (CO_2) and methane (CH_4) in faujasite (FAU)-type zeolites NaX and NaY by performing the grand-canonical Monte Carlo (GCMC) simulations at 288, 298 and 308 K and a pressure range up to 10 MPa. Simulation results have been analyzed using Langmuir and Toth model. Thermodynamic parameters of Gibb's free energy change, entropy change, and enthalpy change were calculated using adsorption equilibrium constant obtained from the GCMC simulations. The results suggested that NaX has higher affinity for both CH4and CO2than NaY and it is more favorable for CO_2 than CH_4 to adsorb in NaX and NaY.

D. Shubo et al. [28] prepared, pine nut shell-derived activated carbons at different KOH/C mass ratios and activation temperatures, and they were used to adsorb CO_2 at different adsorption temperatures and pressures. We should carefully select suitable activated carbons for CO_2 capture according to their micropore distribution and different adsorption conditions.

C. Chao et al. [29] had prepared highly mesoporous LTA zeolite and investigated for CO_2 adsorption. Owing to its mesopores, rapid gas transport inside the zeolite framework was achieved, leading to faster CO_2 adsorption kinetics than that of microporous 4A at 298 K, 1 bar conditions. Mesoporous LTA zeolite also showed CO_2 uptake surpassing that of a micropous zeolite 4A under high pressure ranges (>10 bar), which was attributed to a combined effect of mesopores and large pore volume.

M. M. Hassan et al. [30] have developed a basic dynamic model for a pressure swing adsorption air separation process based on binary Langmuir equilibrium and linearized mass transfer rate expressions. The equilibrium data, using independently measured kinetic and model predictions are matched with experimental results gotten in a simple two-bed air separation pressure swing adsorption (PSA) system filled with a carbon molecular sieve adsorbent.

W. Wangyun et al. [31] presented an important portion of the studies have been dedicated to developing new adsorbents, the invention of best operating conditions and new operating modes is equally and essential important. The current work was aimed at presenting a comprehensive process for developing a correctly tuned numerical model of a fixed-bed adsorption process for carbon dioxide (CO_2) capture using zeolite 13X through parameter estimation.

The key to this development is a related parameter estimation technique and a proposed mass transfer rate model. This paper shows the experimental parameter estimation methods can be applied to adsorption procedures with new adsorbents for carbon dioxide (CO_2) capture.

CHAPTER 3

PROCESS DESCRIPTION

3.1. Introduction

3.2. Process of Cryogenic Air Separation

3.1. Introduction

The atmosphere is of a composition which apart from moisture, fluctuates within narrow limits. The most significant constituents of dry air are shown in the table 3.1;

Table 3.1: Composition of air [35, 36]

Gas	Volume (%)	Weight (%)	Boiling Point (K)	Molar Mass (Mole)
Nitrogen	78.084	75.5	77.35	28.01
Oxygen	20.946	23.1	90.19	32.00
Argon	0.934	1.29	87.27	39.95
Carbon dioxide	0.02-0.04	0.05	194.68	44.01
Rare gases	0.002	-----	---------	-------

99.04% of the air contains O_2 and N_2. The concentration of these gases is less, more or same all over the world. This also applies to argon which contributes with 0.93% by vol. whereas the concentration of H_2 (hydrogen), CO_2 (carbon dioxide) and HC (hydrocarbons) fluctuate within certain limits. The water vapour content of air however varies considerably; this depends on the temperature which is subjected to the degree of saturation, to metrological and local conditions which influence the RH (relative humidity).

H_2O (Water vapour) and CO_2 (carbon dioxide) possess properties which differ considerably from air. These components vaporize at 0°C and -79°C respectively at atmospheric pressure. If these gases were in the process air, the fine tube of the heat exchanger and the perforated trays in the rectification columns would be blocked. These constituents therefore must be removed previous to separating the air. Harmful impurities in the air are acetylene, hydrocarbons. Hydrocarbons (HC) therefore must be removed. The concentrations of acetylene (C_2H_2) in the liquid oxygen should not exceed 0.1 ppm.

Rare gases are chemically fairly non-reactive (inert gases) and, except He and Ne, do not affect with the air separation process. Due to their low boiling points, these two gases will always a gaseous state during air separation. Helium gas pockets forming in the condensers and disturb their functions. Due to this cause, He (helium) is continually vented off through a regulating valve. The difference in the boiling points of the key constituents in the air makes it possible to separate air by distillation column.

The basic principle of the process is to separate liquid air into its various components by cryogenic rectification using the different boiling points of the air gases. For the production of gaseous oxygen the corresponding liquid product is pressurized by pumps, warmed up and evaporated in the main heat exchanger and disturbed to the lines. The nitrogen coming from the low pressure column is warmed up in the main heat exchanger and is further compressed to the required pressure by a turbo compressor [32].

The air separation plant consists of the following parts and sections;

1. Air compression and pre cooling system.
2. Molecular sieve station for the removal of water vapour, most of hydrocarbons and CO_2.
3. Heat exchanger for cooling down the process air closed to its dew point and for warming up the products.
4. Booster compressor for the additional compression of the process air before entering the main heat exchanger.
5. Expansion turbine for the gaseous high pressure flows.
6. Rectifications.
7. Internal compression of oxygen product.
8. External compression of nitrogen gas product.
9. Liquid oxygen, liquid nitrogen and liquid argon storage and backup system.

3.2. Process of Cryogenic Air Separation

The process is shown on the attached process flow sheet.

3.2.1. Air compression

In the mechanical air filter the process air is cleaned from dust and other particles. It is then compressed to the required process pressure by a multistage, intercooled turbo compressor.

3.2.2. Pre-cooling

The process air cooler cool down and washes the compressed air in counter flow with water. There are two streams of water injected into air cooler, cooling water at normal temperature at the lower section and chilled water from evaporation cooler and refrigeration units at the top of air cooler.

The descending cooling water also scrubs the water-soluble chemical impurities from the process air. A wire mesh on top of the process air cooler removes the water mist from the process air. In the evaporation cooler the dry and pressure less nitrogen absorbs part of the

injected cool water. The required heat for the evaporation is provided by the water which is cooled down by this effect. This water is called chilled water. The water losses of this system due to evaporation will be recovered by cooling water out of the cooling water system.

3.2.3. Purification with molecular sieve

The air purification system comprises two cyclic operating adsorber vessels passing through an adsorber vessel, the molecular sieve retains the remaining moisture, CO_2 and potentially hazardous hydrocarbons from the air steam.

While one adsorber is purifying the air, the other adsorber is regenerated. During the heating cycle the regeneration gas (waste nitrogen gas from the coldbox) is heated by an electric heater and desorbs water and CO_2 from the molecular sieve. During the cooling cycle the heater is switched off and the adsorbent is cooled down with cold dry waste nitrogen gas. After the completion of the regeneration sequence, the adsorber is pressurized before being switched over to the adsorption cycle.

The regeneration cycle consist mainly heating, cooling, pressurizing and depressurizing.
The regeneration gas coming from the rectification unit as waste gas is heated up in the regeneration gas electrical heater at heating period. At the cooling period the heater is bypassed. An important indication for sufficient regeneration is the regeneration peak temperature which appears during the cooling cycle. At the end of the regeneration cycle the regenerated adsorber is set into operation and the other one starts with a new regeneration cycle. The cycles are automatically controlled by a program.

3.2.4. Process refrigeration

The main stream of the purified air enters the coldbox. It is cooled down in the main heat exchanger to about liquefaction temperature while the cold gaseous oxygen and nitrogen streams cooling from the column are heated up. The air is feed to the bottom section of the pressure column.

A side steam of the purified air is channelled through the booster heat exchanger. Afterward the stream is split in two. One fraction is further compressed by a multistage intercooled turbo-type air booster compressor while the second one is compressed by the turbine coupled booster compressors with aftercooler. Both streams are cooled down in the booster heat

exchanger and in the main heat exchanger. The turbine boostered stream leaves the main heat exchanger in the middle section and is expanded in the expansion turbine. The gaseous air is fed into the middle section of the low pressure column. A second turbine is on stand-by and can be used during start up to accelerate the cooling down process [33]. The air stream passes the booster heat exchanger. This side stream is then cooled in the main heat exchanger, where it serves as heating medium to evaporate and warm up the internally compressed product (LOX). Downstream the heat exchanger this side stream is expanded into the pressure column by an expansion valve.

3.2.5. Air separation

In the pressure column the air is separated into pure N_2 at the top, and oxygen enriched liquid air at the bottom. The required reflux for the rectification is provided by condensing the gaseous nitrogen in the condenser/reboiler. The condensation heat of the nitrogen is transferred to the boiling oxygen. Part of the liquid nitrogen serves as reflux for the pressure column. The other part is used as reflux for the low pressure column [32, 34]. Part of the N_2 is withdrawn from the top of the pressure column and passes the main heat exchanger before it serves as sealgas for the plant. In the low pressure column the final separation takes place into pure oxygen at the bottom and pure nitrogen at the top. Liquid oxygen from the bottom of the low pressure column evaporates in the condenser/reboiler and rises in the low pressure column. The gaseous oxygen product originates at the bottom of the low pressure column. The oxygen internal compression pump increases the pressure to the required value. The pressurized liquid evaporates and warms up in the main heat exchanger while high pressure air coming from the booster air compressor cools down and liquefies. The oxygen leaves the coldbox as high pressure gaseous oxygen product. Liquid oxygen product is withdrawn at the top of the main condenser and channeled to the oxygen storage system.

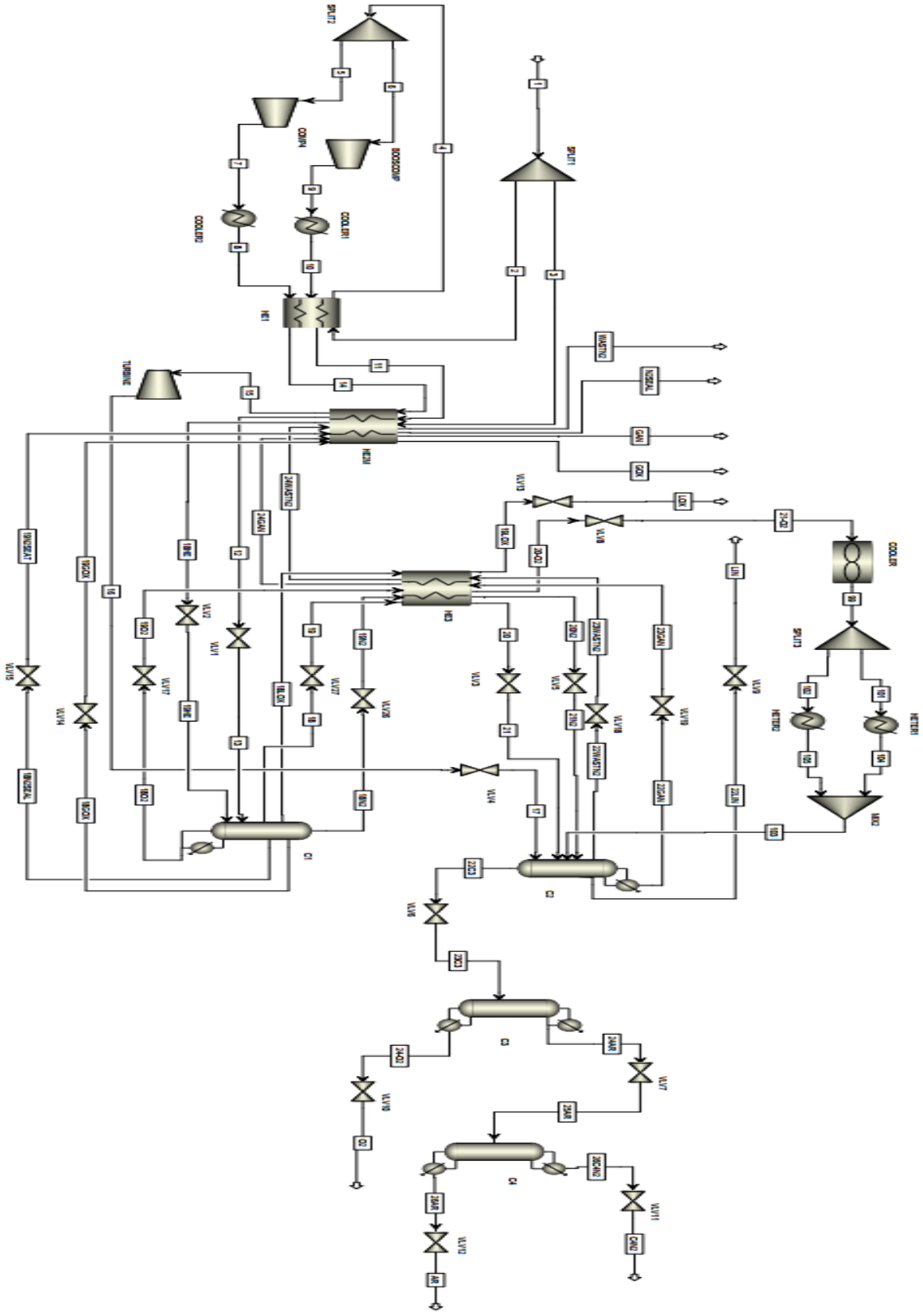

Figure 3.1: Schematic flow diagram of cryogenic air separation plant.

1- C1, C2, C3, C4 are columns, 2 -VLV are valves, 3 –HE1, HE2M, HE3 are heat exchanger.

Liquid nitrogen product is withdrawn at the top of the low pressure column and transferred to the nitrogen storage system. Impure gaseous nitrogen (GAN) from the top of the low pressure column warms up in the sub-cooler and in the main heat exchanger and split into two streams. One stream passes the evaporation cooler in order to produce chilled water for the process air cooler. The remaining part is used as regeneration gas and passes the regeneration gas heater and molecular sieve adsorbers.

3.2.6. Argon production by rectification

In the crude argon column the oxygen is removed from the crude argon by means of cryogenic rectification. Argon enriched gas from the low pressure column is used as a feed for the crude argon column. The oxygen free crude argon on the top of the crude argon column condenses in the crude argon condenser exchanging heat with oxygen enriched liquid from the pressure column. The liquid crude argon serves as reflux. After passing the crude argon condenser part of the oxygen free crude argon is withdrawn at the top of the crude argon column and fed to the middle section of the pure argon column. In the pure argon column the remaining nitrogen is removed by cryogenic rectification. The top gas of the pure argon column liquefies in the condenser against boiling, oxygen rich liquid from the pressure column. The liquid argon serves as reflux for the rectification.

The remaining nitrogen does not condense and is vented from the outlet of the pure argon condenser to atmosphere. Liquid argon from the sump of the pure argon column is evaporated in the pure argon evaporator and fed back to the column. Pure liquid argon is withdrawn as product from the sump of the pure argon column and transferred to the argon liquid storage tank.

3.2.7. Liquid storage and back-up system

The liquid oxygen product withdrawn from the cold box is stored in an atmospheric flat bottom tank. This liquid storage serves as a backup supply of oxygen in case of a plant shut down. The liquid oxygen withdrawn from the tank pressurizes to the required value by means of the backup pumps, evaporates in the hot water bath vaporizer and is fed to the high pressure gaseous oxygen buffer vessels. Additionally a truck filling pump is available to fill liquid oxygen into a truck.

The liquid nitrogen is stored in an atmospheric flat bottom tank from where it is pressurized with the backup pumps and evaporated in the hot water bath vaporizer and is feed to the pressure reducing station where the desired amounts of high- mid- and low pressure GAN can be regulated. A buffer vessel for high pressure gaseous nitrogen is available. The liquid storage serves for backup the supply of pressure nitrogen in case of a nitrogen compressor shut down. Additionally a truck filling pump is available to fill liquid nitrogen into a truck.

The liquid argon is stored in a pressure tank from where it is further pressurized with the backup pumps, evaporated in the LAR backup evaporators and fed to the pressure reducing station. A buffer vessel for high pressure gaseous argon is available. The liquid storage with evaporators serves as gaseous argon supply to the customer. A truck filling pump is available to fill liquid argon into a truck. Additionally liquid argon from the tank can be pressurized, evaporated and bottled into gas cylinders at the available station.

CHAPTER 4

COMPONENTS AND APPLICATION

4.1. Compressors/expansion turbines

4.2. Coolers

4.3. Adsorbers for air

4.4. Heat exchangers (coldbox main part)

4.5. Rectification columns

4.6. Other components

4.7. Gas analyzer applications

4.8. Application

4.9. ASPEN Software

This chapter provides an approach for details of plant components with figure, numerical analysis, process data for simulation of the cryogenic air separation plant, gas analyzer to check percentage of impurities, application of all produced gases and adsorption, and short introduction about ASPEN PLUS software. To describe plant components, this chapter writing their task, design, operation of mode, process data, figure, table, numerical calculation etc. This paper analyzed cryogenic air separation with the help of ASPEN PLUS but you can also use ASPEN HYSIS and CHEMCAD. ASPEN PLUS analysis is used throughout this thesis. At the last of this chapter we present application and introduction of ASPEN PLUS. The following components are listed below:

4.1. Compressor

Air compressor

Task - Compression of process air to the required operating pressure.

Design -The compressor is a three stage centrifugal compressor with intercooler.

Table 4.1: Process data for air compressor

Process gas	Air
Flow rate approx.	4702 kmol/hr
Suction temperature	29°C
Suction pressure	0.986 Bar
Discharge pressure	4.32 Bar
Discharge temp. last stage	60.9°C
Compressor stages	3
Power consumption at shaft	7360 KW

Booster air compressor

Task - Secondary compression (Boostering) of process air to the required operating pressure.

Design - The compressor is a six stage centrifugal compressor with suction filter, intercoolers and after cooler.

Mode of operation - The process air is compressed through all six stages and directed to the main heat exchanger.

Table 4.2: Process data booster air compressor

Process gas	Air
Flow rate approx.	1175.5 kmol/hr
Suction temperature	25°C
Suction pressure	4 bar
Discharge pressure	63.4 bar
Discharge temp. after cooler	31.8°C
Compressor stages	6
Power consumption at shaft	4746.6 KW

Booster compressor connected with expansion turbine

Task - Compression of process air to the required operating pressure/expansion of the compressed process air for the necessary cold production.

Design - The booster compressor is directly driven by the expansion turbine is mechanically connected.

Mode of operation - The compressor serve as a brake for the expansion turbine. The expansion turbine produces coldness by nearly isentropic expansion.

Table 4.3: Process data for booster compressor connected with expansion turbine

Process gas	Air
Flow rate	1175.5 kmol/hr
Inlet pressure	4 Bar
Discharge pressure	6.81 Bar
Inlet temperature	25°C
Discharge temperature	92.9°C
Compressor stage	1
Nominal power	645.194 KW

4.2. Cooler

Process air cooler

Task - Cooling down the process air coming from the main air Compressor before the air inters the molecular sieve adsorber.

Design - The process air cooler is a vertical column containing packing's. The process air is in direct contact with the cooling water and the chilled water. The air inlet is at the bottom and the outlet is at the top. A demister is installed at the air outlet.

Mode of operation - The warm air enters the column at the bottom and rises to the top of the tower. The air cools down by direct contact with the cooling water and chilled water. Packing are installed to increase the contact surface. The chilled water enters the column above the cooling water. The demister on top of the process air cooler removes water droplets from the cool process air. The level of the warm water in the sump of the column is controlled by a level control valve.

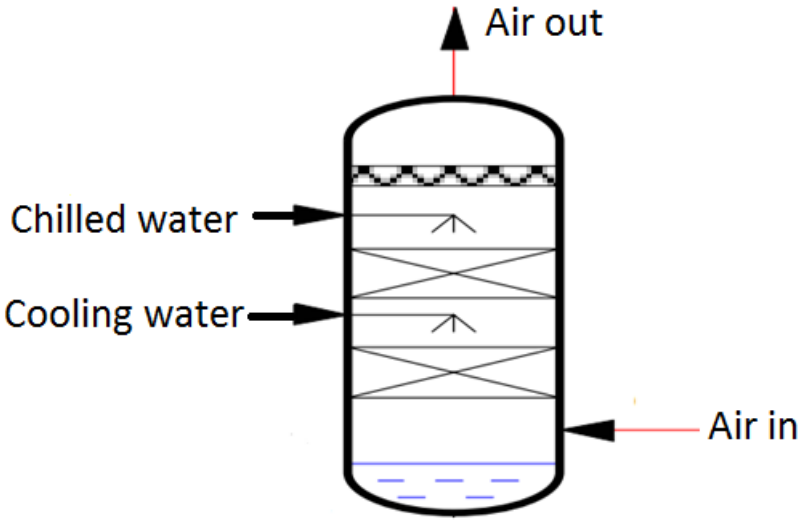

Figure 4.1: Air Cooler

Evaporation cooler

Task - Chilling of cooling water used for the process air cooler.

Design - The evaporation cooler consists of a vessel equipped with packing and a water distribution system. The impure nitrogen enters the vessel at the bottom bellow the packing and leaves at the top. A demister is installed at the top before the outlet.

Mode of operation - The water coming from the cooling water system trickles downwards through the packing in close contact with the rising impure nitrogen. The impure nitrogen which enters the cooler at the bottom is completely dry. When it leaves the evaporation cooler it is saturated with humidity. During the process of evaporation the water chills. It accumulates at the bottom of the cooler and is transferred to the process air cooler by one of the chilled water pumps.

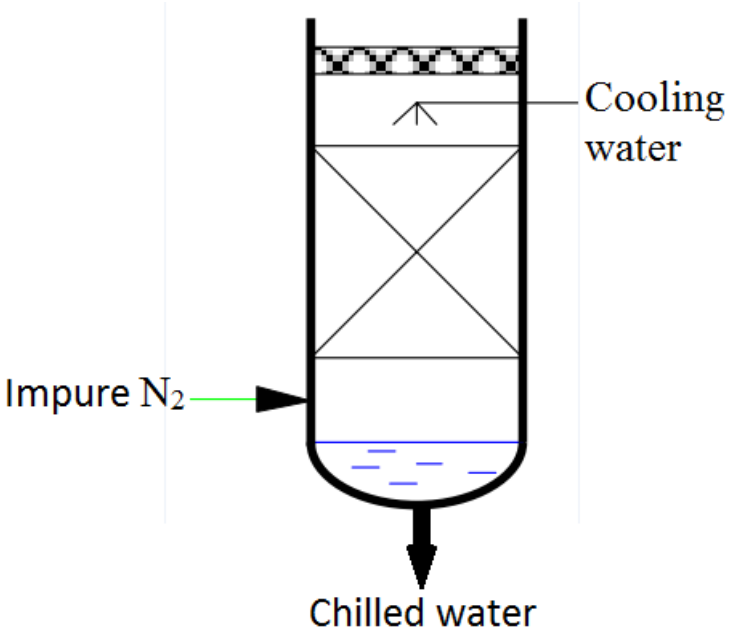

Fig 4.2: Evaporation Cooler

Aftercooler of booster compressor

Task - Cooling of process air after compression in the booster compressors.

Design - Tube heat exchanger

Mode of operation - Heat exchanger between process air and cooling water.

Booster heat exchanger

Task - Heat exchanger between inlet and outlet stream of booster air compressor and booster compressor.

Design - Plate heat exchanger.

Mode of operation - Process air streams coming from compressor and booster compressor are cooled down before entering the coldbox.

4.3. Adsorber

Task - Removal of moisture, carbon dioxide and most of the hydrocarbons from the process air.

Design - The horizontal adsorbers filled with molecular sieve and activated alumina material. The material (adsorbents) can be added and removed through the manholes. The basic design can be seen in the drawing below.

Mode of operation - The molecular sieve adsorber adsorbs the moisture, carbon dioxide and most of the hydrocarbons from the process air. The adsorbents have a limited maximum capacity for these components. It must be generated after a certain time. The adsorber is regenerated by a hot, dry stream of impure nitrogen gas passing the adsorbent revers to the normal flow direction. After regeneration the adsorber must be cooled down with cool gas. Due to their discontinuous mode of operation, adsorbers are always present in pair or multiple units.

Table: 4.4 Operating data for molecular sieve adsorbers

Feed:		
flow rate	kmol/hr	4702
pressure	bar	4.2
temperature	K	303
Operating steps:		
Adsorption time of CO_2	min	267
Adsorption time of H_2O	min	67
Vessel filling: quantity per vessel from bottom to top		
Activated alumina	kg	8400
	m	0.36
Molecular sieve	kg	25450
	m	1.15
Total filling height	m	1.51
Total vessel length	m	8.37
Vessel diameter (inner)	m	4.2
Adsorption pressure drop	mbar	39.8

The adsorption separation is based on three different mechanisms: steric, equilibrium, and kinetic mechanisms. In the steric separation mechanism, the porous solid has pores having dimensions such that it permits small molecules to enter while excluding large molecules from entry. The equilibrium mechanism is based on the solid having different abilities to accommodate different species, that is the stronger adsorbing species is preferentially removed by the solid. The kinetic mechanism is based on the different rates of diffusion of different species into the pore; thus by controlling the time of exposure the faster diffusing species is preferentially removed by the solid [37].

In an adsorption process, as shown in figure 4.3, atoms or ions or molecules, in a liquid or gas diffuse to the surface of solid, where they bond with solid surface. The adsorbent solutes are denoted to as adsorbate, whereas the solid material is the adsorbent [38].

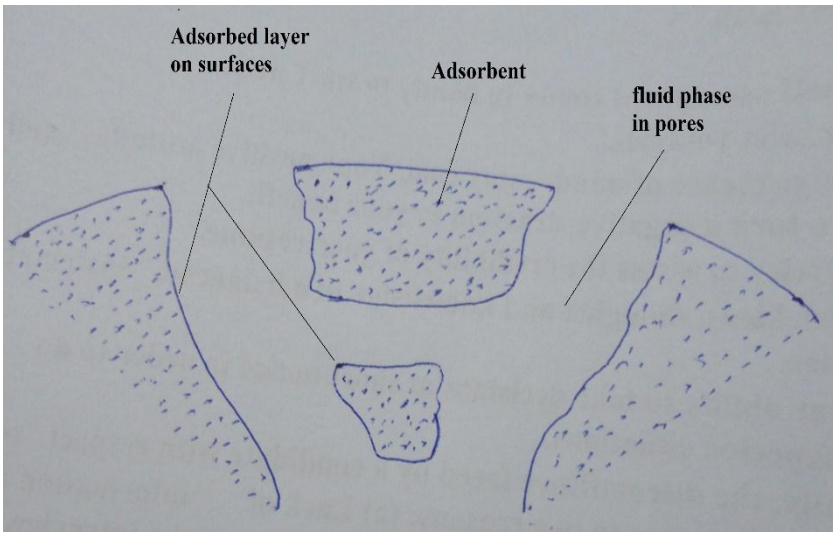

Figure 4.3: Sorption operations with solid-particle sorbents: adsorption.

Molecular sieves are a micro porous material which can selectively adsorb liquids and gases. Gases for which activated alumina is suitable including helium, argon, sulphur dioxide, hydrogen, low molecular weight alkanes, hydrogen chloride, chlorine, fluoroalkanes, and ammonia. Other uses for activated alumina include such as aromatics, kerosene, chlorinated hydrocarbons and gasoline fractions (39).

The arrangement and number which is determined by the factor of fixed beds include total feed flow rate, other energy demands allowable pressure drop, the length of the mass transfer zone, the capital investment and the method of adsorbent regeneration.

4.3.1. Simulation process

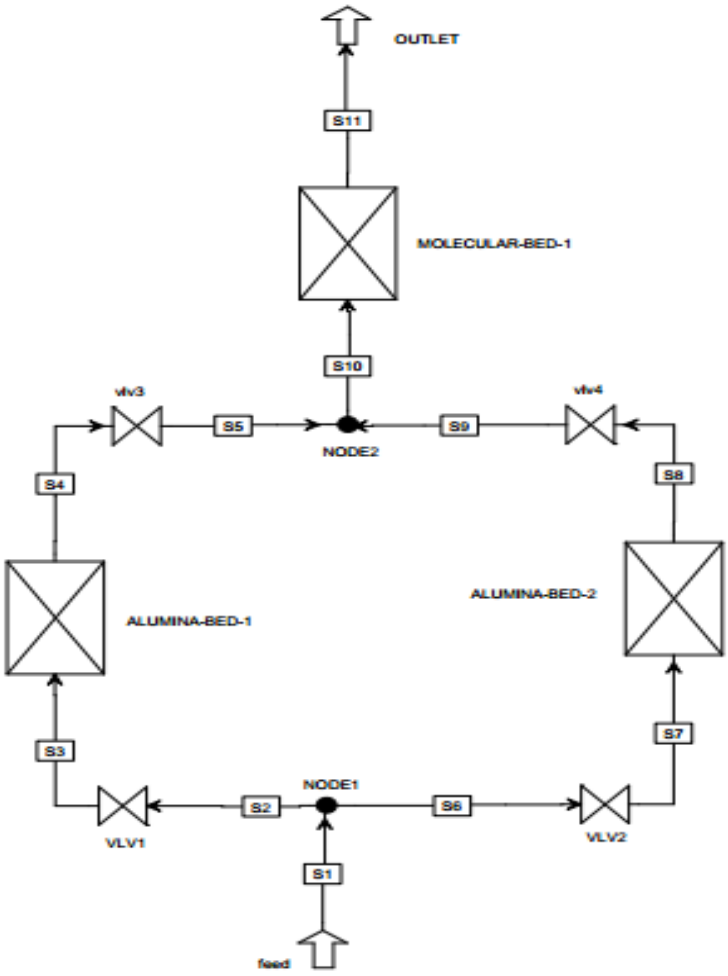

Figure 4.4. The simulated flow chart

4.3.2. Mathematical models and parameters

Mathematical models

The fixed bed adsorption process using isothermal and constant mass transfer coefficient, the specific model assumptions are:

1. The ideal gas law applies.
2. The flow pattern is plug flow model, and radial concentration is same without axial diffusion, besides the pressure drop through the bed conforms to the Ergun equation.
3. The kinetic model Assumption is lumped resistance, the mass transfer driving force for component i is a linear function of the gas phase concentration (fluid film).
4. The adsorption equilibrium is described by toth model for CO2 and by Freundlich 1 model for H_2O.
5. The discretization method is Upwind Differencing Scheme 1 (UDS1).

According to these assumptions the model equations are[23]:

Continuity equation:

$$-\varepsilon_i E_{Zi}\frac{\partial^2 c_i}{\partial z^2}-\varepsilon_i E_{ri}\frac{1}{r}\frac{\partial}{\partial r}(r\frac{\partial c_i}{\partial r})+\frac{\partial(v_g c_i)}{\partial z}+\varepsilon_B\frac{\partial c_i}{\partial t}+j_i=0 \qquad \text{----------4.1}$$

Where， ε_i-bed porosity ($m^3 \cdot m^{-3}$), E -diffusivity coefficient ($m^2 \cdot s^{-1}$), r -bed radius (m), ε_B - total of bed and pellet porosity, v_g -space velocity (m/s), j_i-mass transfer rate ($kmol \cdot m^{-3} \cdot s^{-1}$).

Ergun equation:

$$\frac{\partial p}{\partial z}=\left(\frac{1.5\times10^{-3}(1-\varepsilon_i)^2}{(2r_p\psi)^2\varepsilon_i^3}\mu v_g+1.75\times10^{-5}M\rho_g\frac{(1-\varepsilon_i)}{2r_p\psi\varepsilon_i^3}v_g^2\right) \qquad \text{----------4.2}$$

Where, μ -viscosity ($Ns \cdot m^{-2}$), M - molecular weight ($kg \cdot kmol^{-1}$), ψ -adsorbent sharp factor, r_p - pellet radius (m).

The resistances to mass transfer equation:

$$j_i=MTC_i(c_b-c_s)=-\rho_s\frac{\partial w_i}{\partial t} \qquad \text{----------4.3}$$

Where, j_i is mass transfer rate ($kmol \cdot m^{-3} \cdot s^{-1}$), MTC_i is mass transfer coefficient (s^{-1}), C_i is gas concentration ($kmol \cdot m^{-3}$), C_b is gas-solid interfacial concentration ($kmol \cdot m^{-3}$), Cs is gas concentration ($kmol \cdot m^{-3}$), ρ_s is bulk solid density of adsorbent ($kg \cdot m^{-3}$).

Toth model equation:

$$w_i=\left[\frac{(IP_1C_i)^{IP_2}}{1+(IP_3C_i)^{IP_2}}\right]^{\frac{1}{IP_2}} \qquad \text{----------4.4}$$

Where, IP_1 , IP_2 and IP_3 are parameters of isotherms, C_i is equilibrium concentration ($kmol/m^3$), w_i is adsorption weight ($kmol \cdot kg^{-1}$).

Freundlich modal equation

$$Q_i=IP_{1i}C^{IP_{2i}} \qquad \text{----------4.5}$$

Where IP_1/IP_2 are parameters of isotherms and C_i is equilibrium concentration ($kmol/m^3$)

UDS1 equation:

$$\frac{\partial\Gamma_i}{\partial z}=\frac{\Gamma_i-\Gamma_{i-1}}{\Delta z} \qquad \text{----------4.6}$$

Model parameters

Model parameters used in simulation are listed in below Table[40];

Table 4.5: Model parameters used in simulation of CO_2

Variables	Values	Units	Description
Hb	1.15	m	Height of adsorbent layer
Hb	4.2	m	Internal diameter of adsorbent layer
Ei	0.42	m^3void/m^3bed	Inter-particle voidage
Ep	0.26	m^3void/m^3bed	Intra-particle voidage
RHOs	1597	kg/m^3	Bulk solid density of adsorbent
Rp	1	mm	Adsorbent particle radius
SFac	1.0		Adsorbent shape factor
MTC(CO_2)	6.7	s^{-1}	Constant mass transfer coefficients
IP(1,“ CO_2”)	0.071	Kmol·kg^{-1}·bar^{-1}	Isotherm parameter
IP(2,“ CO_2”)	0.57	Kmol·kg^{-1}·bar^{-1}	Isotherm parameter
IP(3,“ CO_2”)	48.45	Kmol·kg^{-1}·bar^{-1}	Isotherm parameter

Table 4.6: Model parameters used in simulation of H_2O

Variables	Values	Units	Description
Hb	0.36	m	Height of adsorbent layer
Hb	4.2	m	Internal diameter of adsorbent layer
Ei	0.42	m^3void/m^3bed	Inter-particle voidage
Ep	0.26	m^3void/m^3bed	Intra-particle voidage
RHOs	1684.18	kg/m^3	Bulk solid density of adsorbent
Rp	1	mm	Adsorbent particle radius
SFac	1.0		Adsorbent shape factor
MTC(H_2O)	8	s^{-1}	Constant mass transfer coefficients
IP(1,“ H_2O”)	0.41339	Kmol·kg^{-1}·bar^{-1}	Isotherm parameter
IP(2,“ H_2O”)	0.9	Kmol·kg^{-1}·bar^{-1}	Isotherm parameter

4.4. Heat exchanger (coldbox main part)

Counter flow heat exchanger

Task - Heat exchange between two or more gas or liquid streams.

Design - Plate heat exchangers

Plate fin heat exchanger consists of stapled, brazed aluminium plate with spacers. Gas respectively liquid streams are parted in a number of passages which are separated from each other by plane plates.

Mode of operation - The heat exchanger can be used for various applications. The mode of operations of the heat exchangers in this plant is described on the following pages.

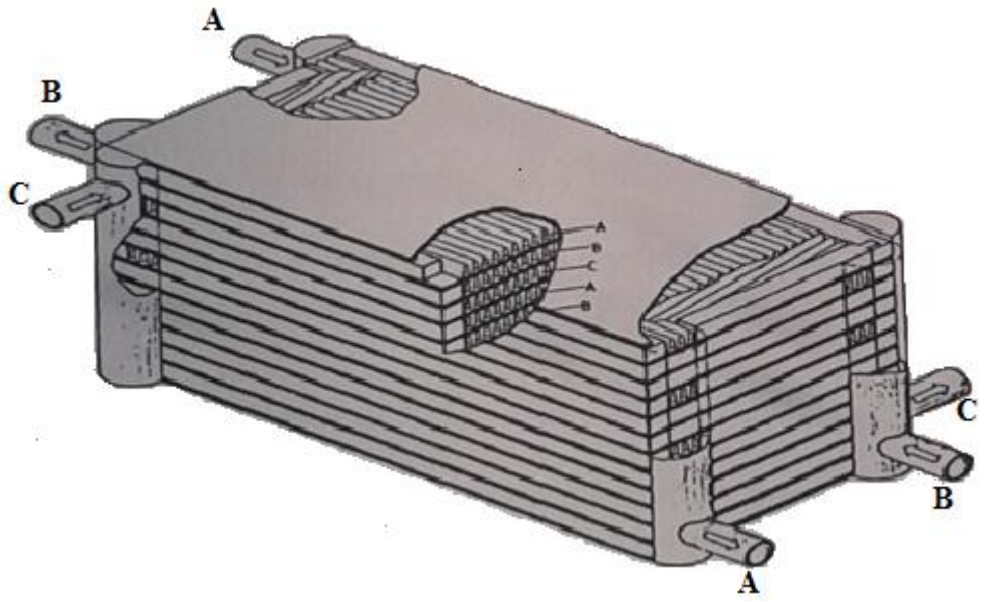

Figure 4.5: Plate fin heat exchanger

Main heat exchanger

Task - Heat exchange between the process air and the various product resp. waste gas streams.

Design - Three heat exchanger blocks. See description for "counter flow heat exchanger" and drawing.

Mode of operation - The process air cools down from about ambient temperature almost to its dew point. The turbine air cools down to an intermediate temperature in order to avoid too much liquefaction in the turbine. At the same time on the opposite side the internally compressed liquid evaporate and warm up to about ambient temperature as well as the cold products and west gas streams.

Subcooler

Task - The task is the sub cooling of liquid air and liquid nitrogen going to the low pressure column in order to reduce the flash portion.

Design - See description for "counter flow heat exchanger" and drawing.

Mode of operation - The cold liquids coming from the pressure column are sub cooled by exchanging heat with the colder waste nitrogen gas coming from the top of the low pressure column. The purpose of sub cooler is to reduce evaporation losses especially during throttling of the cold liquid (flash).

Main condenser cascade type

Task - The condensation of nitrogen gas for the reflux in pressure and low pressure column and the evaporation of liquid oxygen in the sump of the low pressure column.

Design - Cascade condenser with multiple stage. Each stage works as a bath condenser. The partitioning reduces the pressure drop due to the hydrostatic height of the liquid.

Mode of operation - In the following the function of the main condenser is explained by using typical process valves. Pure gaseous nitrogen at 5.2 bar coming from the pressure column enters the main condenser. Liquid oxygen at 1.37 bar from the sump of the low pressure column is pumped to the top of the condenser and flows downwards from stage to stage. As the gaseous nitrogen is supposed to condense while the liquid oxygen evaporates, both streams have boiling point/dew point temperature. With respect to the corresponding pressure the following temperature can be read from the graph "equilibrium of boiling oxygen/nitrogen mixtures" shown below;

$T_{(N2)}$=94.4 K (-178.6°C) for the nitrogen,

$T_{(O2)}$=93.1 K (-179.9°C) for the oxygen,

In this case the temperature difference is sufficient to liquefy the gaseous nitrogen while evaporating the liquid oxygen. The nitrogen contains gas components with low boiling point such as helium. These gases can cover the heating surface when accumulating in the condenser and can hinder further condensation. Therefore a small quantity of gas is removed from the nitrogen part at the relevant point and fed to the waste gas stream.

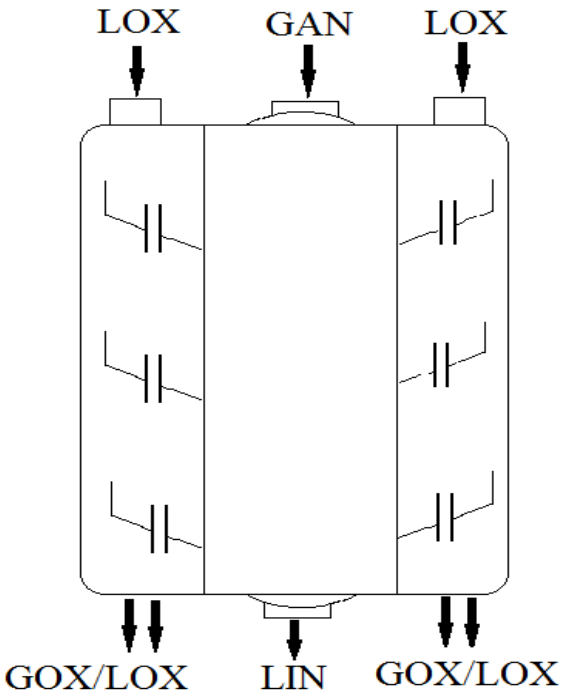

Figure 4.6: Main condenser cascade type

Condenser/reboiler

These condensers/reboilers are bath type condensers with one plate heat exchanger block and work on the same principle as described above.

4.5. Rectification Column

Pressure column, low pressure column, crude argon column, and pure argon column

Task - separation of gas/liquid mixtures into pure components

Design - This column is vertical cylindrical vessels containing packing sections. A packing is made of structured perforated sheets which are arranged in layers. They form intersecting crossing channels. These crossing channels are oblique to the vertical axis of the column. The angle of gradient of the layers is alternately covered.

Mode of operation - The liquid reflux trickles downwards over the surface of the packing in a zigzag downward motion. The total surface and all meshed opening are covered by a thin homogeneous liquid film. Vapour rises upwards through the open channels such as both phases mix. Due to this intensive contact of gas and liquid the components in the liquid with a lower boiling point vaporize while the components in the gas with a higher boiling point condense. The packings lead to a smaller pressure drop than sieve trays.

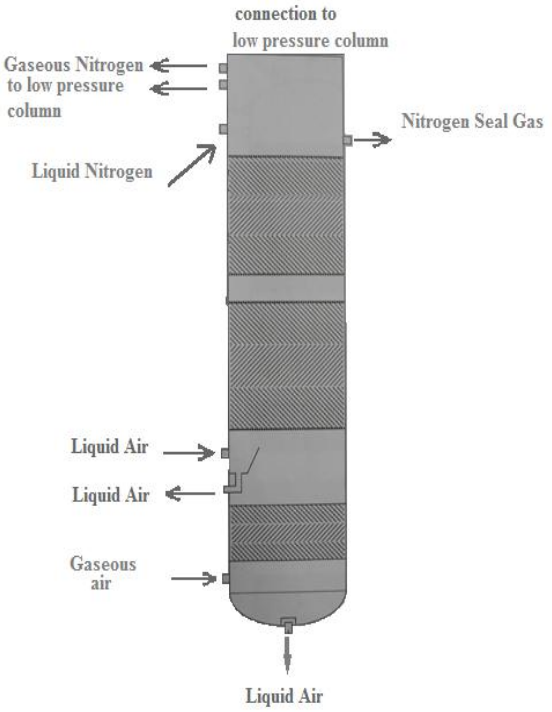

(A)

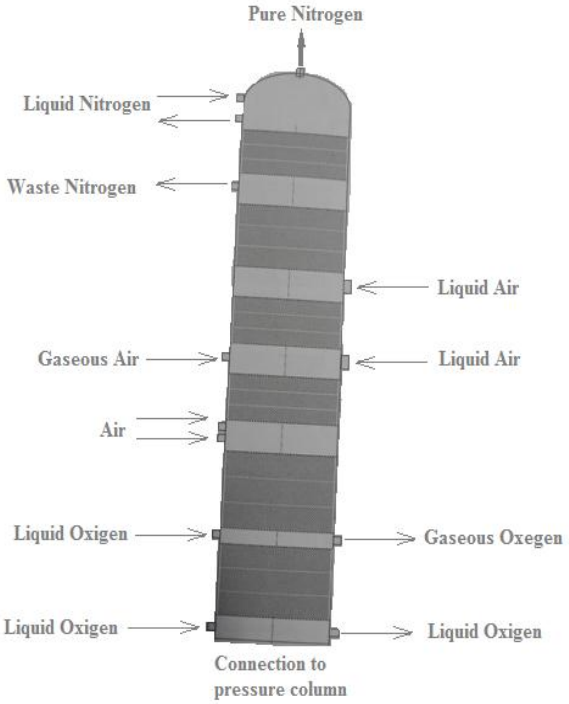

(B)

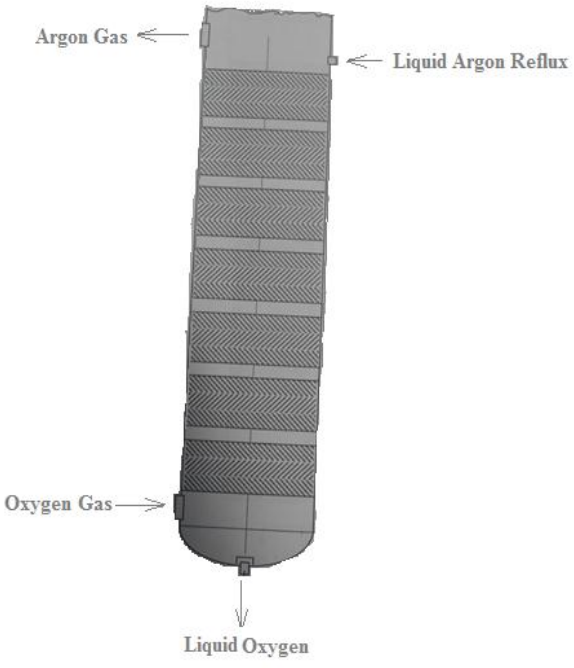

(C)

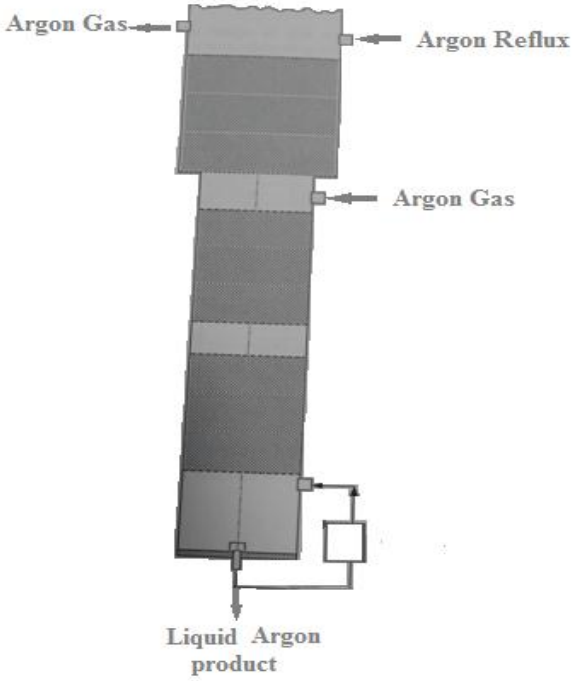

(D)

Figure 4.7: (A) Pressure column, (B) Low pressure column, (C) Crude argon column, and (D) Pure argon column

Structured packing is often preferred over random packing to overcome capacity limitations of trayed towers. Packed-tower performance is often studied on the basis of equivalent equilibrium stage by a packed height equivalent to a theoretical (equilibrium) plate (stage), called the HETP and defined by the equation [38].

$$HETP = \frac{Packed\ height}{number\ of\ equivalent\ equilibrium\ stages} = \frac{l_T}{N_t}$$

4.6. Other components

Process air filter

Task - Cleaning the process air through retaining dust and solid particles.

Design - Course and fine filter pockets dust and solid particles are retained.

Valves (inside coldbox)

Task - Sealing or throttling of gas or liquid streams.

Design – Valve depends on the type of sealing. The valve built into the low temperature section called cold valves, they differ from the normal type of valve and they are made of low temperature material. The following methods of operation can be used to describe the valves:

- Valves operated by manually
- Valves operated by pneumatically
- Valves operated by hydraulically
- Valves operated by electrically

4.7. Application

4.7.1. Application of cryogenics gases

Cryogenic gases are consumed almost in all industries; some are given below in table 4.9.

Table 4.7: Gases (O_2, N_2, Ar) Consuming Industries

Gas	Consuming Industries
Oxygen	Metal, chemical, medical, food, refineries, petrochemical, waste water, semiconductor, aerospace, glass, paper & pulp etc.
Nitrogen	Metal, food, machinery, chemical, medical, refineries, petrochemical, semiconductor, glass etc.
Argon	Metal, machinery, semiconductor etc.

4.7.2. Application of adsorption

Gas purifications:

- Removal of CO_2 from natural gas
- Removal of organics from vent streams
- Removal of NO_x from N_2
- Removal of solvents and odors from air
- Removal of water vapour from air and other gas streams
- Removal of SO_2 from vent streams
- Removal of sulphur compound from gas streams

Liquid purifications:

- Removal of water from organic solutions
- Removal of organic from water
- Removal of sulfur compounds from organic solutions
- Decolorization of solutions

4.8. ASPEN Software

ASPEN is a comprehensive chemical process modeling system, used to design and improve their process plants. ASPEN PLUS is used for steady state process simulation. ASPEN ADSIM is used to simulate adsorber (fixed bed adsorption).

In 1970s, the researchers at MIT's Energy Laboratory developed a prototype for process simulation. They called Advanced System for Process Engineering (ASPEN). This software has been commercialized in 1980's by the foundation of a company named Aspen Tech. ASPEN PLUS offers a complete integrated solution to chemical process industries. This sophisticated software package can be used in almost every aspect of process engineering from design stage to cost and profitability analysis. It has a built- in model library for separators, distillation columns, reactors, heat exchangers, etc. Custom or propriety models can extend its model library. Aspen Plus can interactively change specifications such as, feed compositions, operating conditions, and flow sheet configuration, to analyze process and run new cases alternatives. Aspen Plus allows us to perform a wide range of tasks such as fitting plant data to simulation models, estimating and regressing physical properties, optimizing process, generating custom graphical and tabular output results, and interfacing results to spreadsheets.

CHAPTER 5

RESULT AND DISCUSSION

5.1. Discussion of result for Cryogenic Air Separation unit simulation

5.2. Discussion of result for adsorber

This chapter discusses the simulated result of air separation plant in steady state, purity level of product gases, performance of column, carbon dioxide (CO_2) and water vapour (H_2O) adsorption in adsorber. In this chapter the performance of cryogenic air separation process are summarized and their results are outlined.

5.1. Discussion of result for cryogenic air separation unit simulation

The simulation was performed successfully and results were obtained without any error.

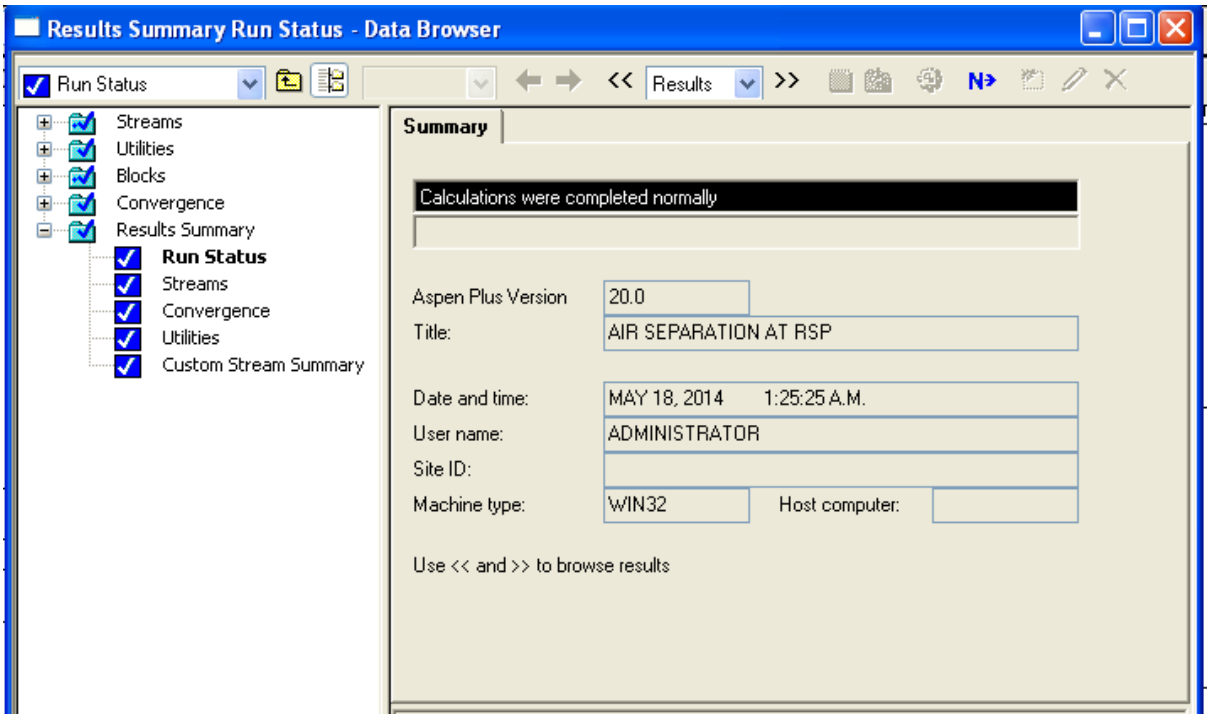

Figure 5.1: Success report of simulation

Figure (3.1) shows the simulation scheme of air separation based on the above described input data. The results of material and enthalpy balance for all product output are shown in Table (5.1). There are some assumption to run ASU;

- Input mode is steady state.
- Valid phases is vapour-liquid.
- Property method: PENG-ROBINSON
- Defined stream class for flow sheet section CONVEN (The simulation does not involve solids, or the only solids are electrolytes salts).
- Solver for sequential modular solution is DMO.

Table 5.1: Streams material result of steady state simulation for Raurkela steel plant.

	WAST N2	N2SEAL	GAN	GOX	LOX	LIN	O2	C4N2	AR
Temperature ° C	-43.6	-43.63	-43.6	-43.6	-185.0	-204.11	-194.1	-208.8	-197.09
Pressure bar	0.32	1.00	0.23	1.00	1.01	0.33	0.17	0.06	0.16
Vapor Frac	1.000	1.000	1.00	1.000	0.000	0.004	0.000	1.00	0.000
Mole Flow kmol/hr	70.00	354	2733	93.00	200.00	250.00	695.40	264	42.599
Mass Flow kg/hr	1964.94	9925.53	76563	2982	6416.0	7007.04	22255	7402.1	1700.1
Enthalpy MMBtu/hr	-0.133	-0.674	-5.18	-0.18	-2.46	-2.965	-8.86	-1.70	-0.457
Mole Flow kmol/hr									
N_2	69.1037	353.26	2732.5	trace	trace	249.22	trace	263.45	<0.001
O_2	0.843	0.0059	0.384	92.28	197.95	0.711	695.03	0.001	0.211
AR	0.0535	0.7321	0.093	0.717	2.045	0.071	0.374	0.5466	42.39
Mole-Frac									
N_2	0.9872	0.998	1.00	trace	trace	0.997	trace	0.998	560 PPB
O_2	0.01204	17 PPM	140 PPM	0.992	0.990	0.003	0.9995	3 PPM	0.005
AR	765 PPM	0.0021	34 PPM	0.008	0.0102	282 PPM	538 PPB	0.002	0.995
Vapor phase									
Volume Flow cuft/min	2455.65	3969.51	133412	1042		9.299		13795	
Vap StdVol 0C cuft/min	923.45	4670.02	36054	1227		12.19		3482.7	
Compressibility	0.999	0.998	1.000	0.998		0.983		0.996	
Heat Cap Ratio	1.402	1.404	1.401	1.405		1.42		1.405	

Simulated air separation unit processing 4702 kmol/hr of air to the basic air components Nitrogen (3667.4037 kmol/hr), Oxygen (985.26 kmol/hr) and Argon (42.39 kmol/hr) was designed. Purity of produced Nitrogen is 99.6 %, Oxygen is 99.4% and purity of Argon is 99.5%.

Atmospheric dry air contains approximately 78% nitrogen, 20% oxygen, and 1% argon and flow rate in simulated air separation unit is 4702 kmol/hr. So our outlet product should be

$$Nitrogen = \frac{4702 * 78}{100} = 3667.56\,\text{kmol/hr}$$

$$Oxygen = \frac{4702 * 21}{100} = 987.42\,\text{kmol/hr}$$

$$Argon = \frac{4702 * 1}{100} = 47.02\,\text{kmol/hr}$$

But we get Nitrogen 3667.4037 kmol/hr, Oxygen 985.26 kmol/hr and Argon 42.39 kmol/hr, so usage value is,

$$usage\ value\ for\ Nitrogen = \frac{3667.4037 * 100}{3667.56} = 99.99\%$$

$$usage\ value\ for\ Oxygen = \frac{985.26 * 100}{987.42} = 99.78\%$$

$$usage\ value\ for\ Argon = \frac{42.39 * 100}{47.02} = 90.15\%$$

I.e. we produce 99.99% Nitrogen, 99.78% Oxygen and 90.15% Argon from atmospheric dry air.

Temperature and composition profile of C1

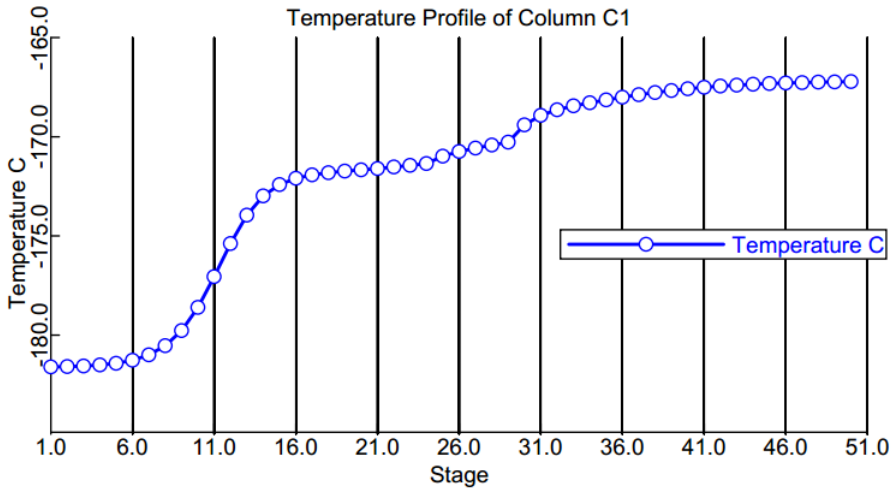

Figure 5.2: Curve between temperature and stage of column C1.

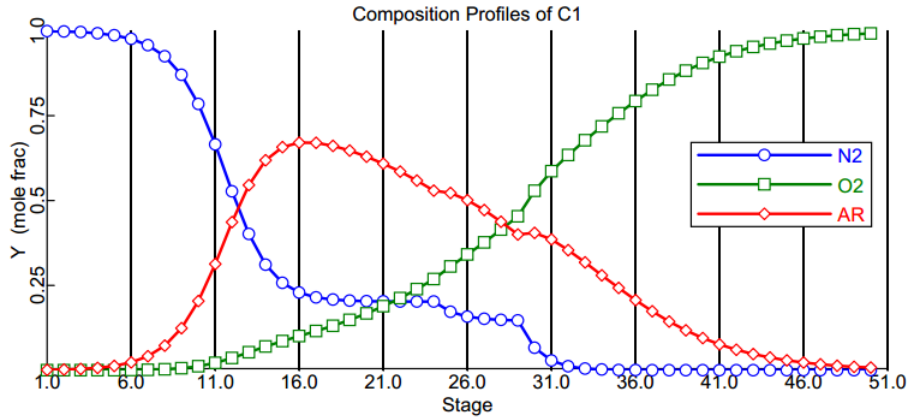

Figure 5.3: Curve between composition and stage of column C1.

Temperature and composition profile of C2

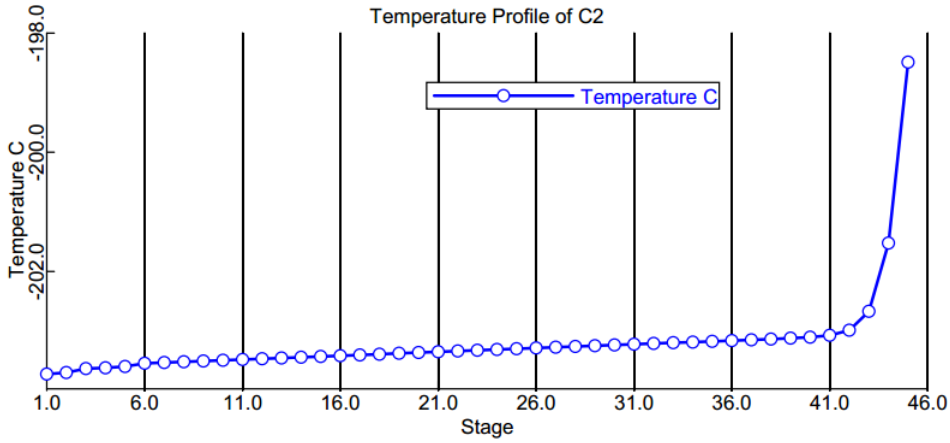

Figure 5.4: Curve between temperature and stage of column C2.

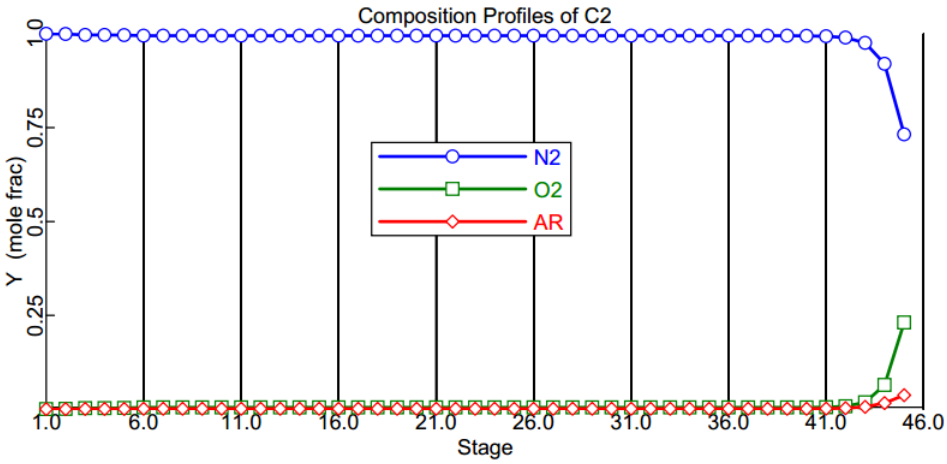

Figure 5.5: Curve between composition and stage of column C2.

Temperature and composition profile of C3

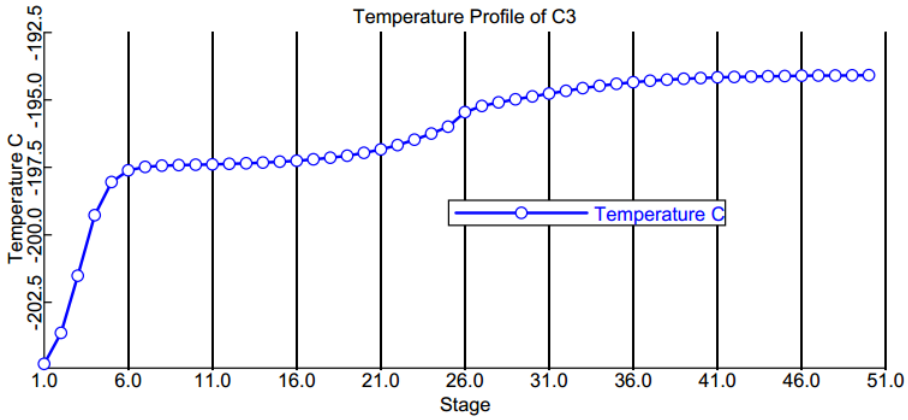

Figure 5.6: Curve between temperature and stage of column C3.

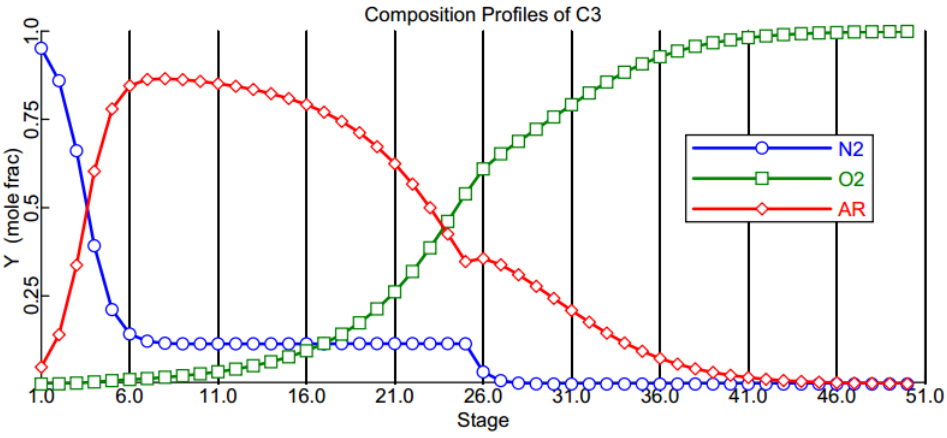

Figure 5.7: Curve between composition and stage of column C3.

Temperature and composition profile of C4

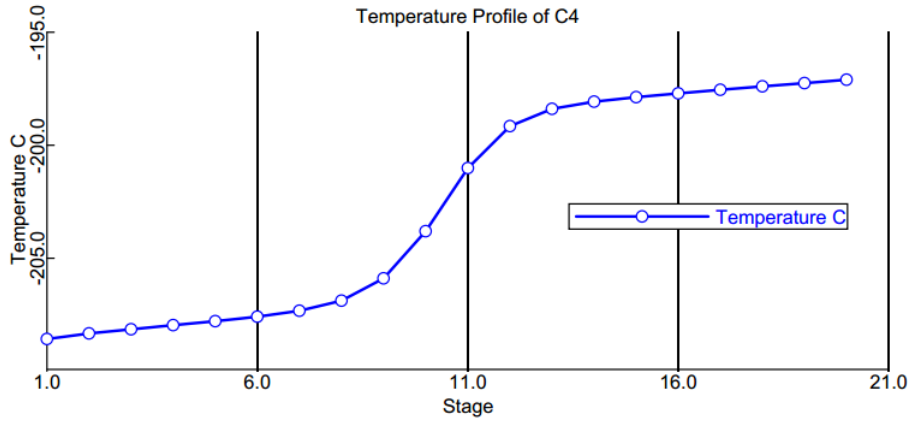

Figure 5.8: Curve between temperature and stage of column C4.

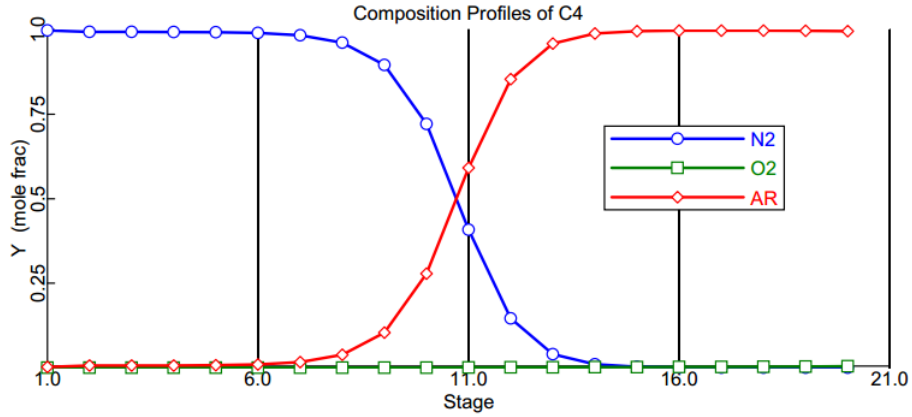

Figure 5.9: Curve between composition and stage of column C4.

In temperature profile, top stage of the column is first stage and bottom stage of the column is last stage, figure 5.2, 5.4, 5.6 and 5.8 shows that temperature increase from top to bottom continuously because of condenser is attached at top and reboiler is at bottom.

In composition profile, top stage of the column is first stage and bottom stage of the column is last stage, figure 5.3, 5.5, 5.7 and 5.9, shows that in the top of the column mole fraction of nitrogen is 100% and oxygen or argon is 0%. As go toward bottom of the column mole fraction of nitrogen is decrease and mole fraction of oxygen or argon is increases continuously.

In composition profile of $C_{4,}$ clearly shows that after stage 15, no use of stage because you will get purity (nitrogen in top and argon in bottom) in stage number 15.

In composition profile of $C_{3,}$ clearly shows that after stage 46, no use of stage because you will get purity (argon in top and oxygen in bottom) in stage number 46.

5.2. Discussion of result for adsorber

5.2.1 Breakthrough curves of CO_2

Breakthrough curve means that the ratio of outlet concentration to the inlet concentration as a function of time. Figure 5.10, shows simulation breakthrough curve of CO_2 on fresh 5A molecular sieve under flow rate of 4702 kmol/hr. Through this curve, find when saturation condition will come. So you can see that at time 267 minute CO_2 will reaches in stable state (saturation condition) then you need to desorption.

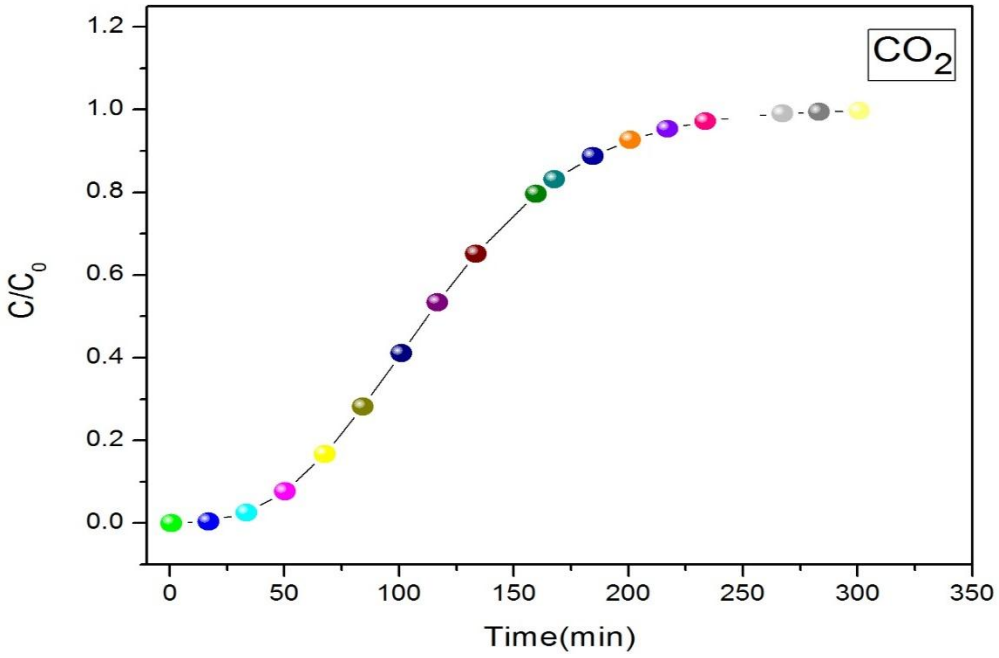

Figure 5.10: Simulation breakthrough curves of CO_2 at outlet

5.2.2 Height Vs Concentration at different time for CO_2

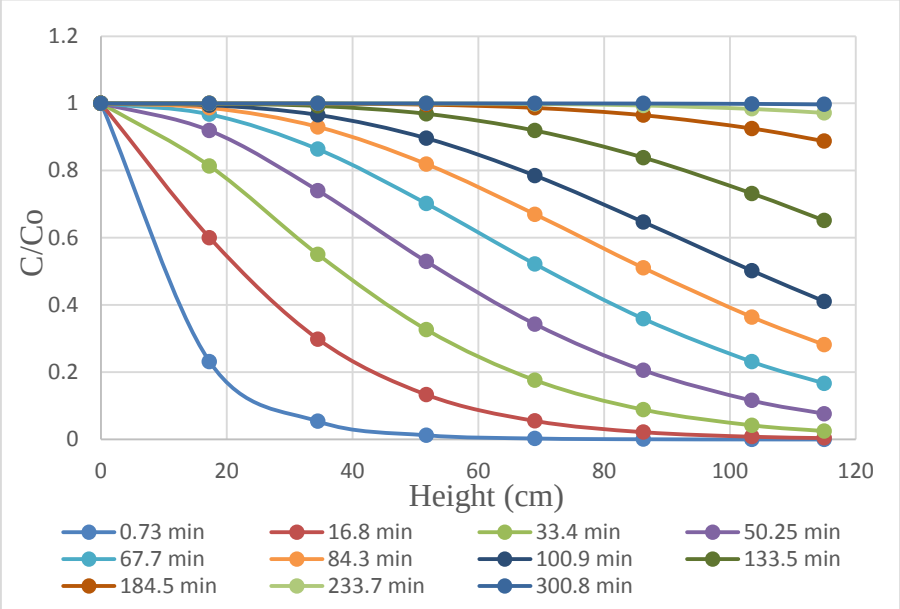

Figure 5.11: Height Vs Concentration at different time

Figure 5.11, shows that concentration of CO_2 decrease with respect to height of bed. So this diagram analyze at different time what is the effect of concentration on height. As time increase then CO_2 concentration come in saturation condition (i.e. CO_2 concentration will increase) but at a particular time CO_2 concentration will decrease on height. At time 267 minute CO_2 come in saturation limit and after that time no use of bed.

5.2.3 Time Vs Concentration at different height for CO_2

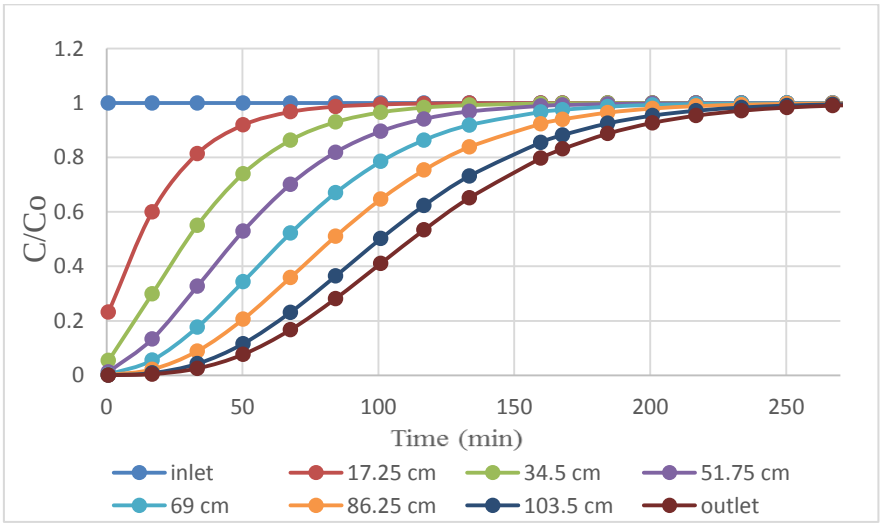

Figure 5.12: Time Vs Concentration at different height

This diagram analyze at different height what is the effect of concentration with respect to time, figure 5.12 shows that as time increase then concentration of CO_2 will increase at different height. At inlet of the bed's porous fill first so they will come in saturation state first and as go toward outlet they will come in saturation state at last. So at outlet of the bed get saturation state in last.

5.2.4. Breakthrough curves of CO_2 under different velocity

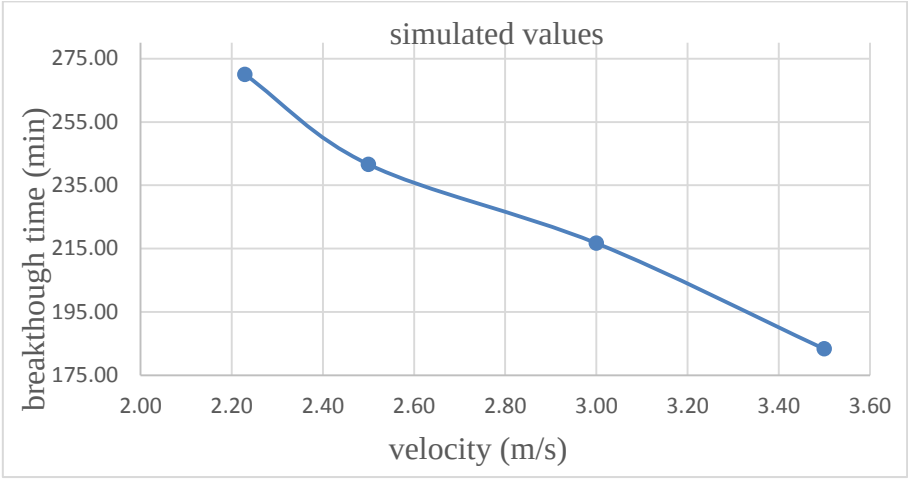

Figure 5.13: Breakthrough curves of CO_2 under different velocity

From figure 5.13 shows that velocity increase then breakthrough time decrease or velocity decrease then breakthrough time increase i.e. breakthrough time is a function of velocity. Reynolds no at velocity 2.22 m/s is (673169), 2.5 m/s (755012), 3 m/s (906015), and 3.5 m/s (1057017)

5.2.5 Breakthrough curves of H_2O

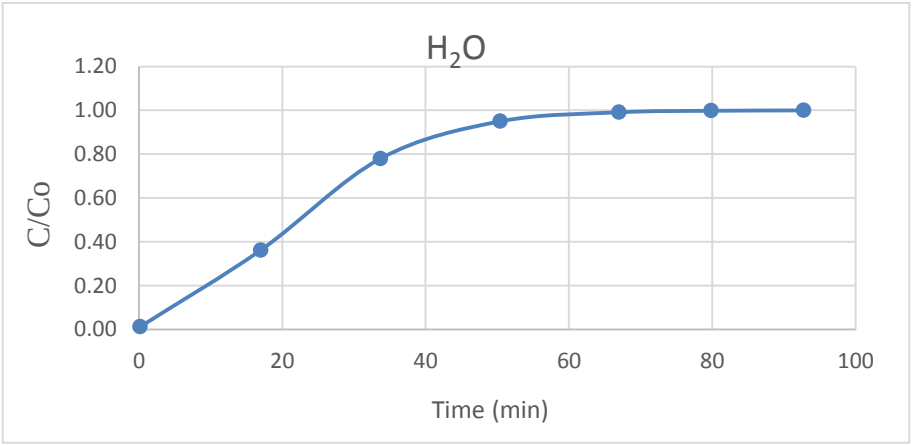

Figure 5.14: Simulation breakthrough curves of H_2O at outlet

Figure 5.14 shows simulation breakthrough curve of H_2O on fresh activated alumina under flow rate of 4702 kmol/hr. So at time 67 minute, CO_2 will reaches in stable states (saturation condition) then you need to desorption.

To absorb carbon dioxide and water vapour, need two bed. Molecular sieve for CO_2 and activated alumina for water vapour. Molecular sieve also used to absorb water vapour but not sufficient. Due to their different saturation time (carbon dioxide 267 minute and water vapour 67 minute), use two activated alumina bed for H_2O and one molecular sieve bed for CO_2 see figure 7. Alumina bed connect in parallel to each other and molecular sieve bed connect in series with alumina bed. First alumina bed is in running condition where second is stand by. After 67 minute second bed is in running condition and first is stand by because after 67 minute, bed come in saturation limit. Outlet from alumina bed feed in molecular sieve bed where carbon dioxide (CO_2) and some remaining water vapour (H_2O) coming from activated alumina bed has absorb. Molecular sieve bed come in saturation condition at 270 minute.

5.2.6 Height Vs Concentration at different time for H_2O

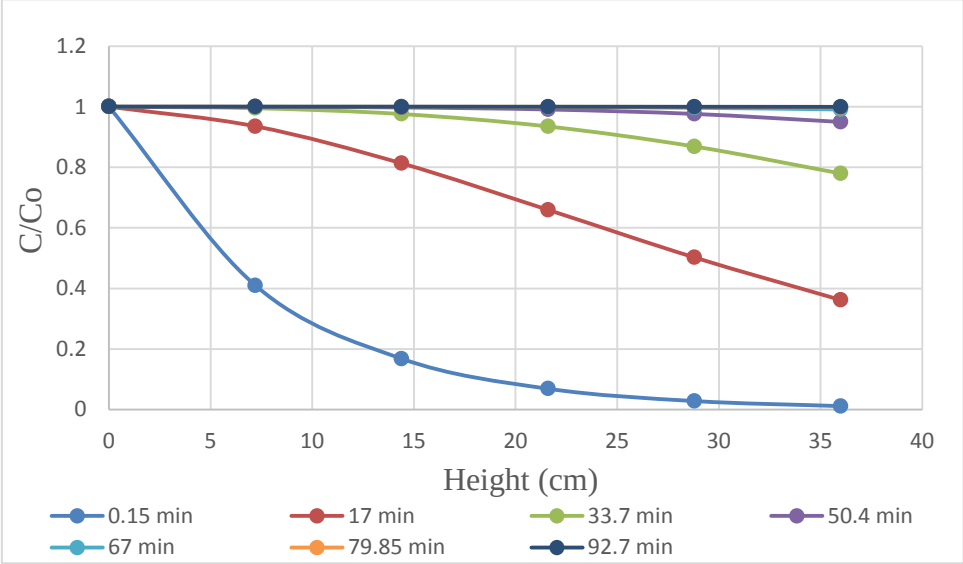

Figure 5.15: Height Vs Concentration at different time

Figure 5.15 clearly shows that concentration decrease with respect to height of bed under different time for H_2O. So analyze at different time what is the effect of concentration of H_2O on height. As time increase then H_2O concentration come in saturation condition (i.e. H_2O concentration will increase) but at a particular time H_2O concentration will decrease on height. At time 67 minute H_2O come in saturation limit and after that time no use of bed.

5.2.7 Time Vs Concentration at different height for H_2O

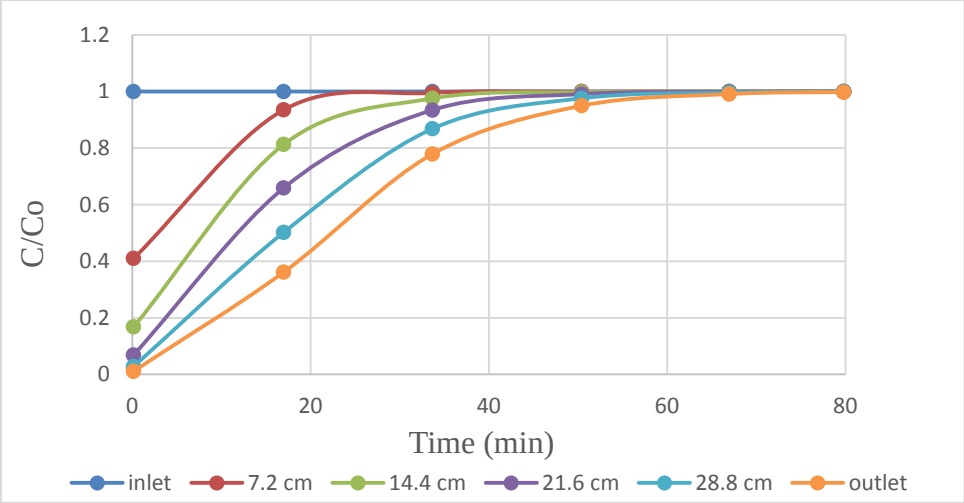

Figure 5.16: Time Vs Concentration at different height for H_2O

Analyze at different height what is the effect of concentration with respect to time, figure 5.16 shows that as time increase then concentration of H_2O will increase at different height. At inlet of the bed's porous fill first so they will come in saturation state first and as you go toward outlet they will come in saturation state at last. So at outlet of the bed get saturation state in last.

5.2.8 Breakthrough curves of H_2O under different velocity

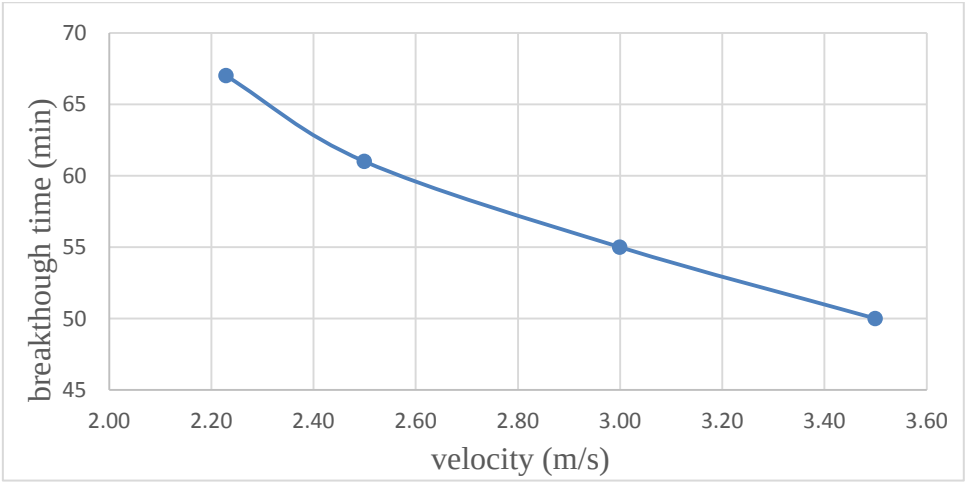

Figure 5.17: Breakthrough curves of H_2O under different velocity

Figure 5.17 shows that as velocity increase then breakthrough time decrease or velocity decrease then breakthrough time increase i.e. breakthrough time is a function of velocity.

CHAPTER 6

CONCLUSION & FUTURE WORK

6.1. Conclusion

6.2. Scope for future work

6.1 Conclusion

From the present work we can summarize the followings;

- In this thesis report, we conclude that an air separation plant processing 4702 kmol/hr of air to the basic air components Nitrogen (3667.4037 kmol/hr), Oxygen (985.26 kmol/hr) and Argon (42.39 kmol/hr) was designed. Purity of produced Nitrogen is 99.6%, Oxygen is 99.4% and purity of Argon is 99.5%. But Rourkela steel plant purity of product nitrogen is 99.99%, oxygen is 99.55% - 99.8% and argon is 99.9%.
- To simulate cryogenic air separation unit, ASPEN Plus software is used.
- At stable states, the breakthrough time of CO_2 is about 267 minute and H_2O is about 67 minute. But Rourkela steel plant breakthrough time of CO_2 and H_2O are 240 minute.
- To adsorb carbon dioxide (CO_2) and water vapour (H_2O), molecular sieve and activated alumina bed are used. Adsorber is simulated through ADSIM of Aspen Tech.

6.2 Scope for future work

Design guideline covers the basic elements of air separation units in sufficient detail to allow an engineer to design an air separation unit with the suitable size of wall thickness, reflux ratio, actual stages, heat duties of a reboiler and a condenser, and permissible pressures [42].The design of air separation may be influenced by factors, including process requirements, economics and safety. A key variability during operation is the price of electricity, which is the dominant operating cost for the process. This work used a steady-state model and assumed perfect control was possible. You can improve the exergy efficiency of a cryogenic air separation unit.

References

[1] Vinson D. R., Air separation control technology, Computers and Chemical Engineering, 30, 1436-1446, 2006.

[2] Smith A.R., Klosek J., A review of air separation technologies and their integration with energy conservation processes, Fuel Processing technology, 70, 115-134, 2001.

[3] Juma H., Tomas P., Steady state and dynamic simulation of crude oil distillation using Aspen Plus and Aspen Dynamics, Petroleum & coal, 51(2), 100-109, 2009.

[4] Liwei Y., Yunsong Y., Yun L., Zaoxiao Z., Energy saving opportunities in an Air separation process, International refrigeration and air conditioning conference at purdue, 2453, 2010.

[5] Agrawal R., Thorogood R. M., Production of medium pressure nitrogen by cryogenic air separation, Butterworth Heinemann Ltd., 5, 203, 1991.

[6] Harry C., Moderate-pressure cryogenic air separation process, Union Carbide Industrial Gases Technology Corp., 5, 25, 1989.

[7] Zhu Y., Sean L., Carl L. D., Optimal operation of cryogenic air separation systems with demand uncertainty and contractual obligations, Chemical Engineering Science, 66, 953-963, 2011.

[8] Zhu Y., Legg S., Carl D. L., Optimal design of cryogenic air separation columns under uncertainty, Computers and Chemical Engineering, 34, 1377-1384, 2010.

[9] Van der Ham L.V., Improving the exergy efficiency of a cryogenic air separation unit as part of an integrated gasification combined cycle, Energy Conversion and Management, 61, 31-42, 2012.

[10] Cornelissen R. L., Hirs G. G., Exergy Analysis of Cryogenic Air Separation. Energy Convers, Energy Convers. Mgmt, 39, 1821-1826, 1998.

[11] Van der Ham L.V., Kjelstrup S., Exergy analysis of two cryogenic air separation processes, Energy, 35, 4731-4739, 2010.

[12] Rizk J., Nemer M., Clodic D., A real column design exergy optimization of a cryogenic air separation unit, Energy, 37, 417-429, 2012.

[13] Chao F., Truls G., Using exergy analysis to reduce power consumption in air separation units for oxy-combustion processes, Energy, 44, 60-68, 2012.

[14] Dustin J., Debangsu B., Richard T., Zitney E. S., Optimal design and integration of an air separation unit (ASU) for an integrated gasification combined cycle (IGCC) power plant with CO_2 capture, Fuel Processing Technology, 92, 1685-1695, 2011.

[15] Nobuaki E., Hiroshi K., Koichi A., Heat and mass transfer model approach to optimum design of cryogenic air separation plant by packed columns with structured packing, Separation and Purification Technology, 29, 141-151, 2002.

[16] Lingyu Z., Zhiqiang C., Chen X., Shao Z., Qian J., Simulation and optimization of cryogenic air separation units using a homotopy based backtracking method, Separation and Purification Technology, 67, 262-270, 2009.

[17] Yasuki K., Akira K., Tsuguhiko N., Atsushi T., A novel cryogenic air separation process based on self-heat recuperation, Separation and Purification Technology, 77, 389-396, 2011.

[18] Zuhua X., Zhao J., Chen X., Shao Z., Qian J., Zhu L., Zhou Z., Qin H., Automatic load change system of cryogenic air separation process, Elsevier Science, 81, 451-465, 2011.

[19] Smith A.R., Klosek J., A review of air separation technologies and their integration with energy conversion processes, Fuel Processing Technology, 70, 115-134, 2001.

[20] Chao F., Gundersen T., Recuperative vapor recompression heat pumps in cryogenic air separation processes, Energy, 59, 708-718, 2013.

[21] Vinson D. R., Air separation control technology, Computers and Chemical Engineering, 30, 1436-1446, 2006.

[22] Li T., Thierry R., Marc B., Production Scheduling Of Air Separation Processes.

[23] Fei Y., Qi L., Wang Y., Zhang L., Cui Q., Wang H., 32Experiment and simulation for the pressure swing adsorption separation of light naphtha.

[24] Jong H. P., Kim J. N., Cho S. H., Kim J. D., Yang R. T., Adsorber dynamics and optimal design of layered beds for multicomponent gas adsorption, Chemical Engineering Science, 53, 3951-3963, 1998.

[25] Manjare S. D. and Ghoshal A. K., Studies on dynamic adsorption behavior of ethyl acetate from air on 5A and 13X Molecular Sieves, The Canadian journal of chemical engineering, 83, 233, 2005.

[26] Rutherford S. W., Do D. D., Adsorption dynamics of carbon dioxide on a carbon molecular sieve 5A, Carbon, 38, 1339-1350, 2000.

[27] Junfang Z., Burke N., Zhang S., Liu K., Pervukhina M., Thermodynamic analysis of molecular simulations of CO_2 and CH_4 adsorption in FAU zeolites. Chemical Engineering Science, 113, 54-61, 2014.

[28] Shubo D., Wei H., Chen T., Wang B., Huang J., Yu G., Superior CO_2 adsorption on pine nut shell derived activated carbons and the effective micropores at different temperatures, Chemical Engineering Journal, 2, 2014.

[29] Chao C., Ahn W. S., CO_2 Adsorption on LTA zeolites - Effect of mesoporosity, APSUSC, S0169-4332(14)01017-4, 2014.

[30] Hassan M. M., Ruthven D. M., Air separation by pressure swing adsorption on a carbon molecular sieve, Chemical Engineering Science, 41, 1333-1343, 1986.

[31] Wangyun W., Lee S., Soon L. K., Modeling and parameter estimation for a fixed-bed adsorption process for CO_2 capture using zeolite 13X, Separation and Purification Technology, 85, 120-129, 2012.

[32] Hring, The Air Gases Nitrogen Oxygen and Argon Industrial Gases Processing, 2007.

[33] Jones D., Optimal design and integration of an air separation unit (ASU) for an integrated gasification combined cycle (IGCC) power plant with CO_2 capture, Fuel Processing Technology, 201109.

[34] Agrawal, Air Liquefaction-Distillation, Encyclopedia of Separation Science, 2007.

[35] Austin G.T., Sherve's chemical industries, Singapore, McGraw Hill Inc., 5th edition, 1984.

[36] Kotz J.C., Treichel P, Chemistry and chemical reactivity, Orlando, USA, Harcourt Brace & Company, 3rd edition, 1996.

[37] Do Duong D., Adsorption analysis-quilibria and kinetics.

[38] Seader J. D., Henley E. J., Separation Process Principles, John Wiley & Sons Inc., USA, 2006.

[39] Barry C., Thomas W. J., Adsorption Technology and Design.

[40] Junfang Z., Burke N., Zhang S., Liu K., Pervukhina M., Thermodynamic analysis of molecular simulations of CO_2 and CH_4 adsorption in FAU zeolites, Chemical Engineering Science, 113, 54-61, 2014.

[41] Egoshi N., Kawakami H., Asano K., Mass transfer in binary distillation of nitrogen-oxygen and argon-oxygen systems by packed column with structured packings, J. Chem. Eng Jpn, 33, 245-252, 2000.

[42] Aprilia J., Air Separation Units (Engineering design guideline), KLM Technology Group, 1-69, 2013.